

Time delay cosmography

Tommaso Treu¹ · Philip J. Marshall²

Received: 15 May 2016 / Published online: 21 July 2016
© Springer-Verlag Berlin Heidelberg 2016

Abstract Gravitational time delays, observed in strong lens systems where the variable background source is multiply imaged by a massive galaxy in the foreground, provide direct measurements of cosmological distance that are very complementary to other cosmographic probes. The success of the technique depends on the availability and size of a suitable sample of lensed quasars or supernovae, precise measurements of the time delays, accurate modeling of the gravitational potential of the main deflector, and our ability to characterize the distribution of mass along the line of sight to the source. We review the progress made during the last 15 years, during which the first competitive cosmological inferences with time delays were made, and look ahead to the potential of significantly larger lens samples in the near future.

Keywords Cosmology · Gravitational lensing · Gravity · Dark energy

1 Introduction

The measurement of cosmic distances is central to our understanding of cosmography, i.e., the description of the geometry and kinematics of the universe. The discovery of the period luminosity relation for Cepheids led to the realization that the universe is much bigger than the Milky Way and that it is currently expanding. Relative distance measurements based on supernova Ia light curves were the turning point in the discovery of the acceleration of the universe (Riess et al. 1998; Perlmutter et al. 1999).

✉ Tommaso Treu
tt@astro.ucla.edu

¹ Department of Physics and Astronomy, University of California, Los Angeles, CA 90095, USA

² Kavli Institute for Particle Astrophysics and Cosmology, P.O. Box 20450, MS29, Stanford, CA 94309, USA

In the two decades since the discovery of the acceleration of the universe, distance measurements have improved steadily. For example, the Hubble constant has now been measured to 2.4 % precision (Riess et al. 2016) while the distance to the last scattering surface of the cosmic microwave background is now known to approximately 0.5 % precision (Bennett et al. 2013; Planck Collaboration et al. 2015, depending on the assumed cosmological model). This precision is more than sufficient for all purposes related to our understanding of phenomena occurring within the universe, like galaxy evolution.

In spite of all this progress, the most fundamental question still remains unanswered. What is causing the acceleration? Is this dark energy something akin to Einstein's cosmological constant or is it a dynamical component? Answering this question from an empirical standpoint will require further improvements in the precision of distance measurements (Suyu et al. 2012; Weinberg et al. 2013; Kim et al. 2015; Riess et al. 2016). In practice, measuring the dark energy equation of state requires an accurate model of the scale parameter of the universe as a function of time, particularly when dark energy is dynamically most relevant, i.e., below $z \sim 1$.

Cosmic microwave background anisotropies primarily provide a measurement of the angular distance to the last scattering surface, obtained by comparing the angular scale of the acoustic peaks with the sound horizon at recombination. Therefore, the constraints set by cosmic microwave background anisotropy data on dark energy parameters are highly degenerate in a generic cosmological model (e.g., Planck Collaboration et al. 2015). Breaking the degeneracy requires strong assumptions about the universe (e.g., flatness or dark energy being the cosmological constant), or lower redshift distance measurements. Many dedicated experiments are currently under way or being planned with this goal in mind.

Precision, however, is not sufficient by itself. In addition to controlling the known statistical uncertainties (precision), modern day experiments need to control systematic errors (accuracy) to fulfill their potential, including the infamous unknown unknowns. The most direct way to demonstrate accuracy is to compare independent measurements that have comparable precision. An interesting, currently topical, and relevant case is that of the $3\text{-}\sigma$ tension between the local distance ladder determination of the Hubble constant H_0 by Riess et al. (2016) and that inferred by the Planck satellite assuming a flat Λ CDM model (Planck Collaboration et al. 2015). The tension could be due to an unknown source of systematic errors in either or both of the two measurements, or it could be indicative of new physics, for example an effective number of relativistic species greater than three. Independent measurements with comparable precision are the best way to make progress. While independent measurements of the same phenomenon, or reanalysis of the same data (Freedman et al. 2012; Rigault et al. 2015; Efstathiou 2014; Spergel et al. 2015), are certainly useful and necessary, completely independent datasets based on different physical phenomena provide qualitatively new information.

Ideally, the comparison between independent measurements should be carried out blindly, so as to minimize experimenter bias. Two mutually blind measurements agreeing that the equation of state parameter w is not -1 would be a very convincing demonstration that the dark energy is not the cosmological constant. Conversely, the

significant disagreement of two blind and independent measurements, could be the first sign of new physics.

In this review, we focus on strong lensing gravitational time delays as a tool for cosmography. As we shall see, this probe provides a direct and elegant way to measure absolute distances out to cosmological redshift. When the line of sight to a distant source of light is suitably well aligned with an intervening massive system, multiple images appear to the observer. The arrival time of the images depends on the interplay of the geometric and gravitational delays specific to the configuration. If the emission from the source is variable in time, the difference in arrival time is measurable, and can be interpreted via a so-called “time delay distance” $D_{\Delta t}$. In the simplest case, this distance is just a multiplicative combination of the three angular diameter distances between the observer, deflector and source. $D_{\Delta t}$ is inversely proportional to H_0 , and more weakly dependent on other cosmological parameters. As several authors have pointed out (Hu 2005; Linder 2011; Suyu et al. 2012; Weinberg et al. 2013), achieving sub-percent precision and accuracy on the measurement of the Hubble constant will be a powerful addition to Stage III and IV dark energy experiments. The independence of time delays from other traditional probes of cosmology makes them very valuable for precise and accurate cosmology. For example, time delays yield an absolute measurement of distance without relying on Cepheids or any other local rung of the distance ladder, and because the relevant quantities are angular diameter distances rather than luminosity distances, the approach is insensitive to dust or other photometric errors.

This review is organized as follows. In Sect. 2, we summarize the history of time delay cosmography up until the turn of the millennium, to give a sense of the early challenges and how they were overcome. In Sect. 3, we review the theoretical foundations of the method, in terms of the gravitational optics version of Fermat’s principle. In Sect. 4, we describe in some detail the elements of a modern time delay distance measurement, emphasizing recent advances and remaining challenges. In Sect. 5, we elucidate the connection between time delay distance measurements and cosmological parameters, discussing complementarity with other cosmological probes. Section 6 critically examines the future of the method, discussing prospects for increasing the precision, testing for accuracy, and synergy with other future probes of dark energy. A brief summary is given in Sect. 7.

Owing to space limitations, we could only present a selection of all the beautiful work that has been published on this topic in the past decades. We refer the readers to recent (Bartelmann 2010; Ellis 2010; Treu 2010; Treu et al. 2012; Jackson 2013, 2015; Treu and Ellis 2015) and not-so-recent (Blandford and Narayan 1992; Courbin et al. 2002; Kochanek et al. 2004; Falco 2005; Schneider et al. 2006) excellent reviews and textbooks (Schneider et al. 1992) for additional information and historical context.

2 A brief history of time delay cosmography

Refsdal (1964) first suggested that strong lens time delays could be used to measure absolute, cosmological distances and, therefore, the Hubble constant to leading order. Unfortunately, no strong lensing systems were known at that time and, therefore, his intuition remained purely theoretical for over a decade.

The prospects of using time delays for cosmography suddenly brightened in the late seventies, with the discovery of the first strongly lensed quasar (Walsh et al. 1979). Even though they were not the strongly lensed supernovae that Refsdal had had in mind, quasar fluxes are sufficiently variable (Vanderriest et al. 1982) that people were able to start to put Refsdal's idea in practice (Vanderriest et al. 1989). The first multiply imaged supernova was discovered in 2014, fifty years after Refsdal's initial suggestion (Kelly et al. 2015), lensed by a foreground cluster of galaxies. The time delays are being measured at the time of writing (Rodney et al. 2016; Kelly et al. 2016); however, it is unclear at the moment whether the cluster potential can be constrained with sufficient accuracy to yield interesting cosmological information (Treu et al. 2016). In general, we expect the more straightforwardly modeled, more numerous galaxy-scale time delay lenses to be the most useful systems for cosmography, with supernovae competing for attention with quasars (Oguri and Marshall 2010).

In this review, we will restrict our case to the hitherto much more common and better understood case of variable active galactic nuclei (AGN) being lensed by foreground elliptical galaxies.

Discovery and monitoring of lensed quasars continued in the 80s and 90s, powered by heroic efforts. By the end of the millennium the number of known strongly lensed systems was in double digits (Courbin et al. 2002), and the first truly robust time delays were measured (Kundic et al. 1997; Schechter et al. 1997). The industrial detection of multiply imaged AGN finally took off at the beginning of the current millennium, with the improvement of panoramic search technology in dedicated or existing surveys (Browne et al. 2003; Oguri et al. 2006; Agnello et al. 2015).

The initial period of time delay cosmography was marred by controversies over systematic errors. The measurement of time delays was particularly controversial during the nineties as the quality of the early data allowed for multiple estimated values (Press et al. 1992), owing to the combined effects of gaps in the data, and microlensing noise in the optical light curves. This problem was solved definitively at the turn of the millennium, with the beginning of modern monitoring campaigns, characterized by high cadence, high precision, and long duration, both at optical and radio wavelengths (Fassnacht et al. 1999, 2002; Burud et al. 2002; Hjorth et al. 2002; Jakobsson et al. 2005; Eigenbrod et al. 2005), as illustrated in Fig. 1. We discuss modern monitoring campaigns in more detail in Sect. 4.1.

Finally, when robust time delays started to become available, the focus of the controversy shifted to the modeling of the gravitational potential of the lens. Typically, in the mid-90s, the only constraints available to modelers were the quasar image positions, time delays, and to lesser extent flux ratios (limited by microlensing, variability and differential extinction). Thus, the best one could do was to assume some simple form for the lens mass distribution, such as a singular isothermal sphere (Koopmans and Fassnacht 1999), and to neglect the effects of structure along the line of sight. As a result of these necessary but oversimplistic assumptions, the apparent random errors grossly underestimated the total uncertainty, leading to measurements that were apparently significantly inconsistent between groups, or with those from other techniques (Kochanek et al. 2004). Since then, two methods have been pursued to obtain realistic estimates of the uncertainties. One consists of using large samples of systems with relatively weak priors (Oguri 2007). The other method consists of obtaining

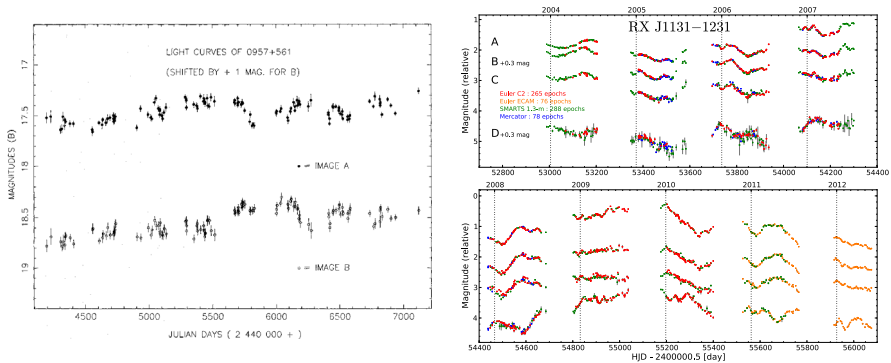


Fig. 1 Comparison between one of the early light curves (*left panel*, from Vanderriest et al. 1989), and a modern light curve from COSMOGRAIL (*right panel*, from Tewes et al. 2013b). Note the improved photometric precision, cadence, and duration of the light curves, allowing for unambiguous determination of the time delay to within 1–2 % precision. Images reproduced with permission from Vanderriest et al. (1989) and (Tewes et al. 2013b), copyright by ESO in both cases

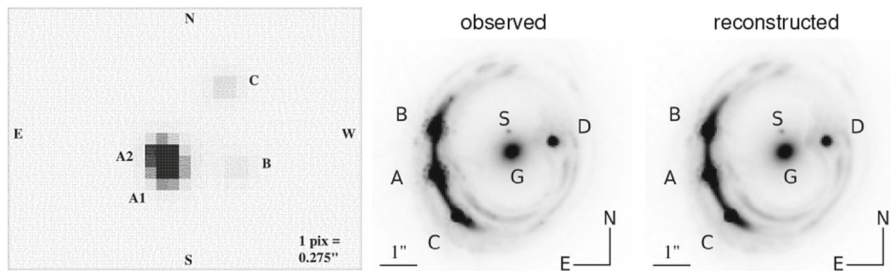


Fig. 2 Comparison between imaging data available in the 90s (*left panel*, from Schechter et al. 1997) and in the most recent studies (*middle and right panels*, from Suyu et al. 2014). With modern data the structure of the quasar host galaxy can be modeled in great detail, providing thousands of constraints on the deflection angle, and thus on the derivatives of the gravitational potential. Images reproduced with permission from Schechter et al. (1997) and Suyu et al. (2014), copyright by AAS in both cases

high-quality data for each lens system, including improved astrometry (Courbin et al. 1997), detailed imaging of the quasar host galaxy (Keeton et al. 2000; Kochanek et al. 2001; Koopmans et al. 2003; Wucknitz et al. 2004; Suyu et al. 2006), or non-lensing data like the deflector stellar velocity dispersion (Treu and Koopmans 2002b) and the properties of galaxies along the line of sight (Keeton and Zabludoff 2004; Suyu et al. 2010). We discuss these approaches in Sect. 4.2. The astounding improvement in data quality over the past two decades is illustrated in Fig. 2.

Ultimately, the controversies over systematic errors were essential to spur the community to overcome the difficulties and find ways to address them. This is a natural and probably inevitable part of the scientific process. However, the bitterness of some of those controversies during the 90s and early noughties still resonates today: unfortunately, some of the scientists that followed the field with excitement at that time are still under the impression that strong lensing time delays are inherently inaccurate and imprecise. As we have briefly described here, and we will show in detail in

the next sections, in the last twenty years the field has moved forward considerably implementing many solutions to the lessons learned the hard way.

3 Theoretical background

In this section, we provide a brief summary of the theory of gravitational lens time delays. We have distilled much of the content of this section from the excellent exposition of [Schneider et al. \(2006\)](#), as well as the various key papers we cite.

Fermat's Principle of Least Time holds for the propagation of light rays through curved spacetime ([Perlick 1990a, b](#)). The light travel time through a single, isolated, thin gravitational lens is given by

$$\tau(\boldsymbol{\theta}) = \frac{D_{\Delta t}}{c} \cdot \Phi(\boldsymbol{\theta}, \boldsymbol{\beta}), \quad (1)$$

$$\text{where } \Phi(\boldsymbol{\theta}) = \frac{1}{2} (\boldsymbol{\theta} - \boldsymbol{\beta})^2 - \psi(\boldsymbol{\theta}). \quad (2)$$

Here, $\boldsymbol{\theta}$ denotes the light source's apparent position on the sky, and $\boldsymbol{\beta}$ is the position of the unlensed source. The difference between the observable position $\boldsymbol{\theta}$ and the unobservable position $\boldsymbol{\beta}$ is the scaled deflection angle $\boldsymbol{\alpha}(\boldsymbol{\theta})$, which is typically ~ 1 arcsecond in a galaxy-scale strong gravitational lens system. $\psi(\boldsymbol{\theta})$ is the scaled gravitational potential of the lensing object, projected onto the lens plane. Both $\boldsymbol{\alpha}(\boldsymbol{\theta})$ and $\psi(\boldsymbol{\theta})$ can be predicted given a model for the mass distribution of the lens.

Images form at the stationary points of the light travel time, where $\nabla \tau(\boldsymbol{\theta}) = \nabla \Phi(\boldsymbol{\theta}) = 0$ ([Schneider 1985](#)). For this reason, $\Phi(\boldsymbol{\theta})$ is known as the “Fermat potential”. This quantity can also be thought of as the spatially varying refractive index of the lens. The arrival time itself is not observable, but differences in arrival time between multiple images are. In the above approximation, the “time delay” $\Delta \tau_{AB}$ between image A and image B can be predicted via

$$\Delta \tau_{AB} = \frac{D_{\Delta t}}{c} \Delta \Phi_{AB} \quad (3)$$

where $\Delta \Phi_{AB}$ is the Fermat potential difference between the two image positions. Figures 3 and 4 illustrate the origin of the time delay between the images in a simple gravitational lens system. The small magnitude of the fractional time delay (typically $\Delta \tau \sim 10$ days out of $D_{\Delta t}/c \sim 10^{12}$ days light travel time) is commensurate with the square of the deflection angle (typically $|\boldsymbol{\alpha}| \sim 1$ arcsecond, or $\sim 5 \times 10^{-6}$ radians). Two characteristic scales are the critical surface mass density Σ_c , and the Einstein radius R_{Ein} . The former is given by a combination of angular diameter distances between the source (s), deflector (d) and observer, $\Sigma_c = 4c^2 D_s / 4\pi D_d D_{ds}$, and it is used to define the dimensionless surface mass density or convergence $\kappa = \Sigma / \Sigma_c$. The latter can be defined, for axisymmetric mass distributions, as the radius of the circle within which the mean convergence $\langle \kappa \rangle = 1$.

We see from Eq. 3 that given a mass model that predicts $\Delta \Phi_{AB}$, we can infer the “time delay distance” $D_{\Delta t}$ from a measured time delay $\Delta \tau_{AB}^{\text{obs}}$. This distance is actually

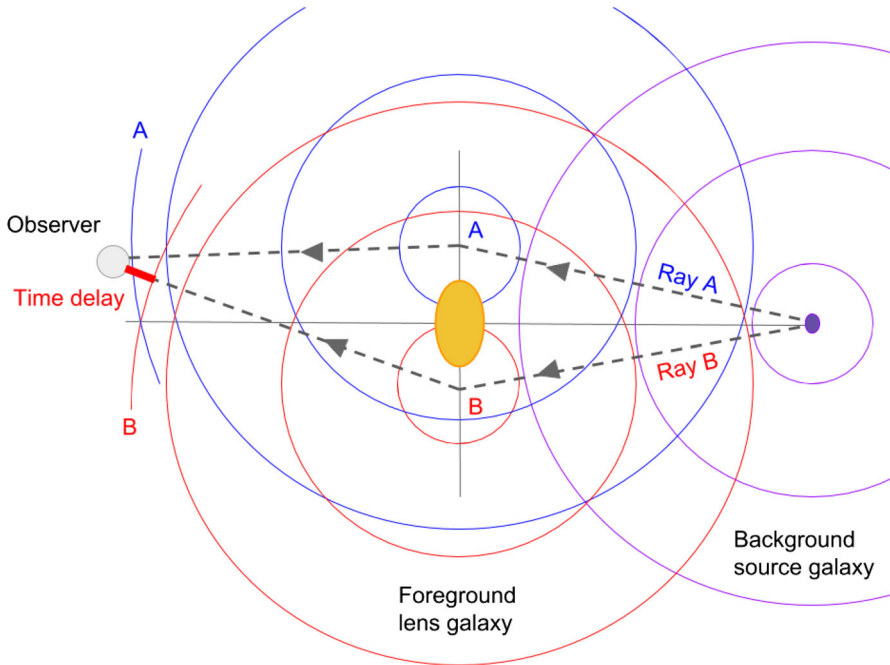


Fig. 3 Schematic diagram illustrating the origin of the geometric component of the time delay

Geometric Delay + Shapiro Delay = Total Delay

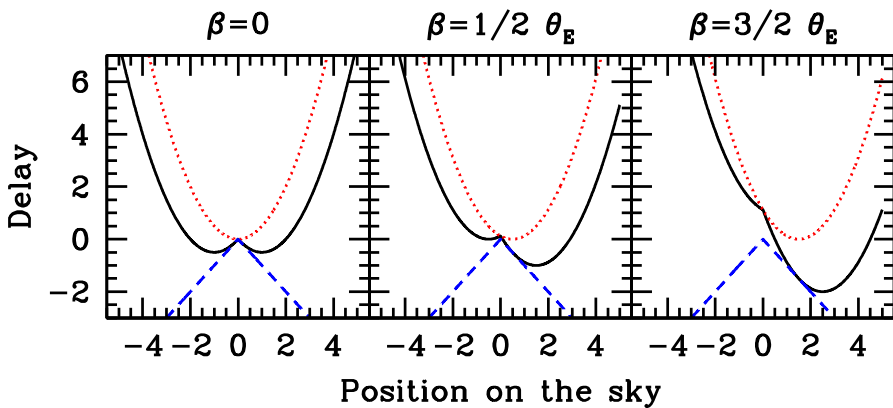


Fig. 4 Geometric and general relativistic (Shapiro) contributions to the lens time delay (Treu and Ellis 2015). Images form at minima and saddle points of the delay surface, shown here in cross section. Different source positions result in different geometrical delays as well as shifted image positions. Image reproduced with permission from Treu and Ellis (2015), copyright by Taylor & Francis

a combination of angular diameter distances:

$$D_{\Delta t} = (1 + z_d) \frac{D_d D_s}{D_{ds}} \quad (4)$$

These angular diameter distances can be predicted given the redshifts of the lens and source, z_d and z_s , and an assumed world model with cosmological parameters Ω . The time delay distance is primarily sensitive to the Hubble constant, since $D_{\Delta t} \propto H_0^{-1}$. All the above formalism pertains to the simple model where all the deflecting mass is arranged on a single lens plane. The multiple lens plane case is more complex, but quantities like $D_{\Delta t}$ appear throughout the equations that predict the time delays, capturing the distances between the lens planes and preserving approximately the same dependence on cosmological parameters (Petters et al. 2001; McCully et al. 2014).¹

Knowledge of the lens mass distribution is of vital importance to the success of this cosmological inference: Eq. 3 shows that the time delay distance is likely to be comparably sensitive to uncertainty in the predicted Fermat potential as it is to the measured time delay itself. More concentrated mass distributions with steeper density profiles produce longer time delays leading to shorter inferred time delay distances, and thus larger inferred values of H_0 (Wucknitz 2002; Kochanek 2002; Suyu 2012).

Moreover, there is significant risk of systematic error when modeling lens mass distributions. While image positions remain invariant under the “mass sheet transformation” (Falco et al. 1985; Schneider and Sluse 2013) (and its generalization, the source-position transformation Schneider and Sluse 2014), the time delays predicted by the model can change significantly. The mass sheet transformation and its effect on the time delay is as follows:

$$\kappa(\theta) \rightarrow \kappa(\theta)' = (1 - \lambda) + \lambda\kappa(\theta) \quad (5)$$

$$\Delta\tau \rightarrow \Delta\tau' = \lambda\Delta\tau. \quad (6)$$

This means that if we allow our model the freedom to generate both the $\kappa(\theta)$ and $\kappa(\theta)'$ mass distributions, our image position data will not favor one over the other: they will be equally likely given the data. This model degeneracy can be broken by additional information.

Perhaps the best sources of additional information are independent measurements of the mass distribution: stellar kinematics is the obvious choice (Koopmans et al. 2003). Another way to break degeneracy is to obtain non-lensing information about the lensed source absolute size (Sonnenfeld et al. 2011) or luminosity (Kolatt and Bartelmann 1998; Holz 2001). This way requires special circumstances, and, therefore, we focus on deflector kinematics in the remainder of this review.

Building on previous work (Grillo et al. 2008; Paraficz and Hjorth 2009), Jee et al. (2015) provide a derivation of the resulting cosmological dependence of kinematics-constrained power law lens galaxy mass models with isotropic orbits, showing that were its density profile and velocity isotropy to be known exactly, a time delay lens would provide a measurement of the angular diameter distance to the lens, D_d , in addition to the time delay distance of Eq. 4. The reason given is that the velocity dispersion and the time delay are both proportional to the enclosed mass of the lens, but depend differently on galactocentric radius: combining the measured velocity

¹ Additional distance dependencies appear in the multi-plane formalism, but always as dimensionless ratios with weaker cosmological dependence. The inverse proportionality to the Hubble constant is the same as in the single plane case.

dispersion and time delay gives a characteristic physical scale of the lens galaxy. The image separation provides a corresponding angular scale, allowing the angular diameter distance to be probed.

In practice, the same mass model must be used to predict all of the measured velocity dispersion, Einstein ring appearance, and time delay data, self-consistently. In the limit of low precision in the velocity dispersion, the profile slope is weakly constrained by the ring image alone, and the combination of time delay and lens mass model provides information on $D_{\Delta t}$ but none on D_d . As the velocity dispersion precision increases, we expect the profile slope to be pinned down, and the angular diameter distance to be constrained as well. In the context of a cosmological model, the two distances are not independent: the angular diameter distance information provided by the velocity dispersion measurement should translate into higher precision inference of the cosmological parameters (Jee et al. 2016). We return to this in Sect. 6.1 below.

Another way to break degeneracy in the lens model is to include prior knowledge of the lens mass distribution from measurements of other galaxies similar to the lens, or perhaps from numerical simulations. This type of information is typically encoded as a simply parametrized model, such as an elliptically symmetric mass distribution with power law density profile (as opposed to a free-form density map; see discussion in Sect. 4.2). Assuming a specific density profile partially breaks the mass sheet degeneracy: how much systematic error in the time delay that assumption introduces is an important topic for research.

The form of the mass sheet transformation given by Eq. 5 is a rescaling plus an offset. One way to achieve such a transformation is, therefore, to change the overall mass of the lens (by a factor of λ), and at the same time add a “mass sheet,” a constant convergence ($1 - \lambda$). Both these variations are possible in nature: lens galaxies come in a range of masses, and the combined gravitational lensing effect of all the other galaxies, groups and filaments along the line of sight to the source can, in the weak lensing limit, be approximated by a constant “external convergence” (which is associated with an “external shear”, capable of further distorting the lensed images). However, these physical effects only complicate the modeling problem, as one is not allowed to assume that the mass density profile of the deflector should vanish exactly at large radii. The physical effect should not be confused with the mathematical degeneracy between lens model parameters that is associated with the mass sheet transformation, and which would be present regardless of any external weak lensing effects. Having said that, any additional external physical mass component must also be taken into account when modeling the lens.

In summary, independent information about the physical mass of the deflector galaxy, such as the kinematics of its stars, can play an important role in breaking the degeneracy in the mass model, which must be able to predict self-consistently the strong lensing effects (image distortions and time delays) and the internal dynamics of the lens galaxy, and take into account the weak lensing effects of structures along the line of sight. Schneider and Sluse (2013) provide demonstrations of the scale of this problem: very good data (both imaging and spectroscopic), as well as physically meaningful assumptions and careful treatment of the models used, will be needed to obtain accurate results. In Sect. 4.2, we review the recent choices and approximations that have been made when constructing such models.

4 Modern time delay distance measurement

Since 2010, it has been recognized that accurate cosmography with individual lens systems involves the following key analysis steps.

Time delay estimation The light curve extracted from monitoring observations is used as input to an inference of the time delay between the multiple images.

Lens galaxy mass modeling High-resolution imaging and spectroscopic data are used to constrain a model for the lens galaxy mass distribution, which can be used to predict Fermat potential differences. Both the Einstein ring image and the stellar velocity dispersion are important.

Environment and line of sight modeling Additional observational information about the field of view around the lens system is used to account for the weak lensing effects due to massive structures in the lens plane and along the line of sight.

Cosmological parameter inference can then proceed—although in practice, the separation between this final step and the ones above is not clean. Practitioners aspire to a joint inference of lens, source, environment and cosmological parameters from all the data simultaneously, but have to date broken the problem down into the above steps. In the next three sections we describe the current state of the art, limitations, and principal sources of systematic error of these three key measurement parts of the problem.

4.1 Measuring time delays

The measurement of gravitational time delays involves two steps: taking observations to monitor the system over a period of several years, and then inferring the time delays between the multiple images from these data.

4.1.1 Monitoring observations and results

Active galactic nuclei (AGN) show intrinsic time variability on many scales, with the variability amplitude increasing with timescale. Long and regular monitoring campaigns can build up high statistical significance as more and more light curve features can be brought into play. However, such long campaigns are difficult to carry out in practice, because a large number of guaranteed, evenly spaced observing nights are required (even if the total exposure time is modest). Scheduling such a program has proven difficult in traditional time allocation schemes, due to the competing demands of the rest of the astronomy community and the long duration requirements of lens monitoring. The highest precision time delays have come from monitoring campaigns carried out with dedicated facilities so far, i.e., observatories that were either able to commit to the long-term monitoring proposal submitted, or that were actually operated in part by the monitoring collaboration.

Monitoring of the CLASS lens B1608 + 656 in the radio with the Very Large Array enabled the breakthrough time delay measurements of [Fassnacht et al. \(2002\)](#).

In its first season, this program yielded measurements of all three time delays in this quadruple image system with precision of 6–10 % (Fassnacht et al. 1999); with the variability of the source increasing over the subsequent two seasons, Fassnacht et al. (2002) were able to reduce this uncertainty to 2–5 %. Such high precision was the result of a dedicated campaign which consisted of 8-month seasons, with a mean observation spacing of around 3 days. The light curves were calibrated to 0.6 % accuracy.

While time delays had previously been measured in ten other lens systems, this was the first time that all the delays in a quad had been obtained; moreover, it brought the time delay uncertainty below the systematic uncertainty due to the lens model, prompting new efforts in this direction beyond what Koopmans and Fassnacht (1999) needed to do.

While B1608 + 656 is not the only radio lens with measured time delays, a combination of factors led the observational focus to shift towards monitoring in the optical. With the sample of known, bright lensed quasars increasing in size, networks of 1–2 m class optical telescopes began to be investigated. The variability in these systems is somewhat more reliable, and while microlensing and image resolution present observational challenges, the access to data was found to be less restrictive. The COSMOGRAIL project (Courbin et al. 2005) took on the task of measuring lens time delays with few percent precision in this way: Eigenbrod et al. (2005) showed that microlensing was likely not to be an insurmountable task, and Vuissoz et al. (2007) provided the proof of concept with a 4 % precision time delay measurement in SDSS J1650 + 4251.

One of the keys to the success of this program has been the simultaneous deconvolution of the individual frames in the imaging dataset, using a mixture model to describe the point-like quasar images and extended lens and AGN host galaxies (Magain et al. 1998). Another is the dedicated nature of the network of telescopes employed, and the careful calibration of the photometry across this distributed system. Seasons of 8–12 months duration over campaigns of up to 9 years have been achieved, with typical mean observation gaps of around 3–4 days.

The COSMOGRAIL team and their collaborators have now published high-precision time delays in WFIJ2033 – 4723 (Vuissoz et al. 2008, 3.8 %), HE0435 – 1223 (Courbin et al. 2011, 5.6 %), SDSS J1206 + 4332 (Eulaers et al. 2013, 2.7 %) and RXJ1131 – 1231 (Tewes et al. 2013b, 1.5 %), and SDSS J1001+5027 (Rathna Kumar et al. 2013, 2.8 %), with more due to follow. Typically multiple years of monitoring are needed to obtain an accurate time delay, as the variability fluctuates and the reliability of the measurement converges (see the discussion in e.g. Tewes et al. 2013b). High-precision optical time delays are also being obtained by other groups (Poindexter et al. 2007; Fohlmeister et al. 2007; Dahle et al. 2015) using similar strategies on different telescopes.

A consistent picture seems to emerge from modern monitoring projects: high-precision gravitational time delay measurement requires campaigns consisting of multiple, long seasons, with around 3-day cadence. The baseline observing strategy for the large synoptic survey telescope (LSST) is somewhat different to this, with seasons expected to be around 4–5 months in length, and gaps between observation nights only reaching 4–5 days when images in all filters are taken into account. The “Time Delay Challenge” project was designed to test the measurability of lens time delays

with such light curves (Dobler et al. 2015), in a blind test offered to the astronomical community. From the ten algorithms entered by seven teams, it was concluded that time delay estimates of the precision and accuracy needed for time delay cosmography would indeed be possible, in ~ 400 LSST lensed quasar systems (Liao et al. 2015). This result came with two caveats: (1) the single-filter light curve data presented in the challenge are representative of the multi-filter data we actually expect, and (2) that “outliers” (catastrophic time delay mis-estimates) will be able to be caught during the measurement process. A second challenge to test these assumptions is in preparation.

4.1.2 Lightcurve analysis methods

How were the time delays surveyed in the previous section derived from the light curve data? Interest in this particular inference problem has been high since the controversies of the late 90s. Fasnacht et al. (1999) used the “dispersion method” of Pelt et al. (1996), a technique that involves shifting one observed light curve relative to another (both in time and in amplitude) and minimizing the dispersion between adjacent points in the resulting composite curve. Uncertainties were estimated by Monte Carlo resampling of the data, assuming the minimum dispersion time delay and magnification ratio to be true. To take into account the slowly varying incoherent microlensing signals present in their optical light curve data, the COSMOGRAIL team have investigated three analysis techniques that all involve interpolation of the light curves in some way (Tewes et al. 2013a): free-knot splines, Gaussian processes and simple linear interpolation have all been tested, within a common “python curve-shifting” (PyCS) framework.² These agree with each other given light curves of sufficient length, providing an argument for multiple-season monitoring campaigns.

The time delay challenge prompted seven analysis teams to develop and test algorithms for time delay estimation. These are outlined in the TDC1 analysis paper of Liao et al. (2015), but we give a very brief summary here as well, along with updated references. The PyCS team tried a two-step approach (visual inspection and interactive curve shifting, followed by automated analyses based on spline model regressions for the AGN variability and the microlensing), and submitted an entry after each step (Bonvin et al. 2016). Two other teams applied similar curve-shifting approaches: both Aghamousa and Shafieloo (2015) and Rathna Kumar et al. (2015) devised smoothing and cross-correlation schemes that they find to be both fast and reliable. Jackson applied the dispersion method of Pelt et al. (1996), but carefully supervised via visual inspection to check for catastrophic failures. The three remaining teams used Gaussian processes (GPs) to model the light curves. Tak et al. (2016) used a custom Gibbs sampler to infer the hyper-parameters describing the GP for the AGN variability and polynomials for the microlensing signals, although they ignored microlensing during the challenge itself. Romero-Wolf and Moustakas implemented a very similar model, also ignored microlensing, and used a freely available ensemble sampler for the inference. Hojjati and Linder (2014) used GPs for both the AGN and microlensing

² The COSMOGRAIL curve-shifting analysis code is available from <http://cosmograil.org>.

variability, and marginalized over their hyper-parameters when focusing on the time delay.

Two factors were important in the minimisation of catastrophic time delay mis-estimation: explicitly including microlensing in the model, and visual inspection of the results. An additional promising avenue for future challenges ought to be ensemble analysis, to exploit (1) the intrinsic correlations between, for example, AGN variability, color and brightness, and (2) the fact that the cosmological parameters are common to all lens systems.

4.2 Modeling the lens mass distribution

In addition to time delays, the second main ingredient entering the determination of time delay distances is the mass model of the main deflector. In the early days of time delay cosmography, one could only rely on the relative positions of the multiple images as constraints (since in general the flux ratios are affected by micro- and millilensing, variability, and differential dust extinction, and are, therefore, highly uncertain). Even for a quadruply imaged quasars, the five positional constraints and three independent delays are insufficient to determine Fermat potential differences to the desired level of precision and accuracy.

There are two classes of solution to the problem of underconstrained lens models. One is to analyze large samples of lenses with physically motivated priors and exploit the fact that cosmological parameters are the same for all lenses to remove model degeneracies. A number of attempts along these lines have been made (Oguri 2007; Rathna Kumar et al. 2015), and it is easy to imagine that this solution will be popular in the future, when large samples of lenses with measured time delays will be available.

The alternative solution is to increase dramatically the number of empirical constraints per lens system by means of dedicated high-resolution imaging and spectroscopic observations (Suyu et al. 2010, 2013, 2014). We describe this approach in detail below.

For simplicity, in this section we describe only the case of a single deflector in a single plane, leaving line of sight and environmental effects for a later section. For clarity, we describe each step corresponding to a different dataset individually. Ideally, all the data, including the time delays, should be modeled holistically at the same time—although in practice the problem has, to date, been broken up into parts to make it more tractable.

4.2.1 High-resolution imaging observations

Lensed quasars reside in a host galaxy. For typical redshifts of lens and source, the host galaxy apparent size is of order arcseconds. Images with sufficient depth and resolution to isolate the bright point source and detect the lower surface brightness host galaxy often reveal extended lensed features connecting the point-like images themselves (e.g., Fig. 2).

In the best conditions, these images cover hundreds if not thousands of resolution elements. The distortion of the detailed features of the lensed images are a direct

measurement of the variation of the deflection angle between the images. In principle, for data with infinite signal-to-noise ratio and resolution one could imagine integrating the gradient of the deflection angle along a path between a pair of images to obtain the difference in Fermat potential, up to a mass sheet transformation (Sect. 3). In practice, in the presence of noisy data and limited resolution, forward modeling approaches have been the most successful so far, as discussed below. From an observational point of view, it has been demonstrated that images with $0.1'' - 0.2''$ FWHM resolution provide good results, provided that the point spread function can be appropriately modeled or reconstructed as part of the lens model itself. The Hubble Space Telescope in the optical/near infrared (Suyu et al. 2010, 2013, 2014; Birrer et al. 2015a) and the Very Large Baseline Interferometer in the radio (Wucknitz et al. 2004) have been the main sources of images for this application. Recent progress in adaptive optics imaging at the 10 m W.M. Keck telescope (Chen et al. 2016), the beautiful data being obtained for lensed source by ALMA (Hezaveh et al. 2013b), and the many facilities currently being constructed or planned (Meng et al. 2015) indicate that the prospects to scale up the number of systems with available high-resolution images are bright.

4.2.2 Lens modeling techniques

Conceptually, a detailed model of a lensed quasar and its host galaxy needs to describe three different physical components: (i) the surface brightness of the source; (ii) the surface brightness of the deflector; (iii) the gravitational potential of the deflector. It is useful to conceptualize the problem in this way, to understand where the information needed to break the degeneracy in the interpretation of the data comes from. Lensing is achromatic and preserves surface brightness so any feature that belongs to the source (including in line of sight velocity Hezaveh et al. 2013a) should appear in all the multiple images (appropriately distorted). Likewise, the deflector is typically a massive early-type galaxy with smooth surface brightness distribution and approximately uniform colors (except for dust, see, e.g., Suyu et al. 2010).

Each of the three components is typically described in terms of one or both of the following choices: (i) simply parametrized functions such as a Sersic profile for the surface brightness of the lens or the source, and a singular isothermal ellipsoid for the gravitational potential of the deflector (e.g., Marshall 2007; Kneib et al. 2011; Keeton 2011); (ii) as combinations of basis sets like surface brightness pixels, lens potential pixel values, or Gauss-Hermite (“shapelet”) functions (e.g., Coles 2008; Birrer et al. 2015a; Nightingale and Dye 2015; Tagore and Jackson 2016). Very flexible models require regularization to avoid overfitting the noise in the data.³ Hybrid approaches have been proposed where the parametrization of some of the components is simple and others are complex (Warren and Dye 2003; Treu and Koopmans 2004; Brewer and Lewis 2006; Suyu et al. 2006; Suyu and Halkola 2010), or where flexibly parametrized “corrections” are added to simply parametrized models (Koopmans 2005; Vegetti and

³ In the case of the shapelet basis set, regularization can effectively be achieved through choosing the number of basis functions to use as well as the scale of the underlying Gaussian. Most analyses using shapelets have taken this approach to date, with Tagore and Jackson (2016) being a notable exception. A promising alternative scheme would be to assign a less physically motivated prior for the shapelet coefficients.

Koopmans 2009; Suyu et al. 2009; Birrer et al. 2015a). The variety of approaches in the literature reflects the inevitable tensions between the need to impose as many physically motivated assumptions as possible, while retaining sufficient flexibility to obtain a realistic estimate of the uncertainties and avoid introducing biases by asserting incorrect simplistic models. If the model is too constrained by the assumption it will lead to underestimated errors, if it is more flexible than necessary it will lead to a loss of precision.

Once the choice of modeling parametrization is set, exploring the posterior PDF for the parameters is numerically non-trivial, often requiring weeks to months of computing time. Fortunately, there are techniques to speed up the calculations by limiting the number of non-linear parameters. For example, for a given lens model, the transformation between source and image plane can be described as a linear operation, or the pixelated corrections to the potential can be found by linearizing the lens equation (see references above).

Ideally, modeling choices should be explored systematically as well, since they can potentially introduce systematic errors. This is currently being done in the most advanced studies, at great expense in term of computing time and investigator time. As we discuss in Sect. 6, speeding up the modeling phase and reducing the investigator time per system will be key to analyzing the large statistical samples expected in the future.

4.2.3 The role of stellar kinematics

As introduced in Sect. 3, stellar kinematics provide a qualitatively different input and are, therefore, very valuable in breaking degeneracies in the interpretation of lensing data (e.g., the mass sheet degeneracy Koopmans et al. 2003), and in estimating systematic uncertainties. Of course, translating kinematic data into estimates of gravitational potential has its own uncertainties and degeneracies (e.g., the mass anisotropy degeneracy for pressure supported systems, or projection effects Gavazzi 2005; Newton et al. 2011; Sonnenfeld et al. 2012; Courteau et al. 2014) but the combination of the two datasets in the context of a single mass model has been proven to be very effective (Treu and Koopmans 2002a, 2004). Even a single measurement of stellar velocity dispersion, interpreted via simple spherical Jeans modeling, has been shown to substantially reduce modeling uncertainties (Treu and Koopmans 2002b; Koopmans et al. 2003; Suyu et al. 2014). It is clear that getting spatially resolved kinematic data will enable breaking the mass-anisotropy degeneracy (see, e.g., Courteau et al. 2014, and references therein) and thus better constraints on the lens model and consequent cosmological inference (Agnello et al. 2016, in prep).

4.3 Lens environments and line of sight effects

The analysis of B1608 + 656 by Suyu et al. (2010) explicitly took into account the weak lensing effects of external structures. Such a correction had been suggested by Fassnacht et al. (2006), who identified 4 galaxy groups along the line of sight in a spectroscopic survey of the B1608 + 656 field; the authors estimated that these

groups could, if left unaccounted for, bias any inferred Hubble constant high by around 5 %, an amount consistent with more general theoretical predictions (Bar-Kana 1996; Keeton and Zabludoff 2004). Further surveys have quantified the environments and line of sight density structures of many more systems (Momcheva et al. 2006; Auger et al. 2007; Wong et al. 2011; Momcheva et al. 2015). Exactly how to model the weak lensing contamination of strong lens signals has been the topic of a number of papers since 2010: the problem is how to incorporate our knowledge of where the galaxies are along the line of sight without introducing additional bias due to the necessary assumptions about how their (dark) mass is distributed, and how the rest of the mass budget in the field adds up.

Suyu et al. (2010) attempted to solve these problems by comparing the B1608 + 656 field with a large number of fields with similar galaxy number overdensity drawn from the Millennium Simulation, modeling the line of sight effects with a single external convergence parameter and accepting a somewhat broad prior distribution for it, in return for not having to make strong assumptions about the structure of the galaxy groups in the field. The external convergence in the simulated fields was calculated by ray-tracing by Hilbert et al. (2009), and the comparison in galaxy overdensity was enabled by the analysis of galaxy number counts in archival HST images by Fassnacht et al. (2011), who found that the B1608 + 656 field was overdense by a factor of two. The resulting prior PDF for the κ_{ext} parameter had median 0.10 with the 68 % credible interval spanning 0.05–0.18. In the analysis of RXJ1131, Suyu et al. (2013) also took into account the inferred external shear from the lens model when deriving the prior for κ_{ext} , noting a significant improvement in precision (as well as a marked shift in the PDF centroid).

Since these initial analyses, a number of improvements have been suggested and investigated. All have in common the desire to bring more information to bear on the problem, to increase the precision (while continuing to avoid introducing bias). Greene et al. (2013) showed that weighting the galaxy counts by distance, photometric redshift and stellar mass can significantly reduce the uncertainty in κ_{ext} , by up to 50 %. Collett et al. (2013) claim an additional 30 % improvement by including knowledge of the stellar mass to halo mass relation in galaxies, and modeling each galaxy halo's contribution to κ_{ext} individually in a 3-D reconstruction of the mass in the field which is then calibrated to simulations in something like the high-resolution limit of the number counts approach. McCully et al. (2014) showed how to compute the weak lensing contamination accurately, using a full multi-plane lensing formalism (see also Schneider 2014) but with fast approximations for less important structures (McCully et al. 2016).

While research into these methods continues, one problem in particular remains outstanding. The methods that involve calibration to numerical simulations are dependent on the cosmological parameters assumed in that simulation, while all methods involve modeling line of sight structures at various distances as part of an evolving universe, whose dynamics depend on cosmological parameters. We face two options: either treat these cosmological parameters self-consistently as hyper-parameters in a joint analysis of the time delays and the lens environments, or demonstrate that they can be decoupled via various simplifying assumptions that introduce sub-dominant systematic error. At the moment, comparison between the results of independent sys-

tems (Suyu et al. 2013) seems to suggest that this source of uncertainty is smaller than the estimated random uncertainty. However, this issue will have to be addressed in detail as the sample sizes increase and the random uncertainty decreases.

5 From time delay distances to cosmological parameters

Early approaches to inferring cosmological parameters from time delay lens observations focused on measuring the Hubble constant in a Friedman–Robertson–Walker model with asserted (fixed) density parameters.⁴ With better data came the recognition that time delay lenses were really probes of cosmological distance (Koopmans et al. 2003; Suyu et al. 2010), and the emphasis shifted to inferring the set of cosmological parameters that are needed to predict the kinematics of the expansion of the Universe out to the redshift of the source. The parameter most strongly constrained is still the Hubble constant, but as sample sizes increase we expect ensembles of lenses to support the inference of several cosmological parameters (or combinations thereof Lewis and Ibata 2002).

In Fig. 5, we reproduce the current constraints on cosmological parameters, from the two best measured systems, B1608 + 656 and RXJ1131 (Suyu et al. 2014). When this figure was made, the available precision from just these two lenses was about the same as that from SDSS DR7 baryonic acoustic oscillations (BAO Percival et al. 2010) or the “Constitution” set of Type Ia supernovae (Hicken et al. 2009). When all three of the curvature density Ω_k , Dark Energy density Ω_{DE} and equation of state w_0 parameters are allowed to vary, along with H_0 , we see that the time delay lenses provide similar constraints to BAO and complementary constraints to the SNe: the time delays and the BAO signal depend on angular diameter distances and H_0 , while the supernovae probe relative luminosity distances.

One important feature of the cosmological parameter inference carried out in the RXJ1131 analysis of Suyu et al. (2013) is that it was blinded. Following the simple methodology suggested in the blind Type Ia supernova analysis of Conley et al. (2006), all cosmological parameter PDFs were plotted with centroids offset to the origin until the team agreed (after notably lengthy discussions about systematic errors) to “open the box,” just before publication.⁵ Such attempts to avoid “unconscious experimenter bias” introduced by stopping systematics analysis when the “right answer” is obtained have long been advocated in particle physics (Klein and Roodman 2005), and seem likely to become the standard in cosmology as well (e.g., Heymans et al. 2006; The Dark Energy Survey Collaboration 2015). It is also crucial to repeat the measurements using independent codes, assumptions, and techniques, to quantify associated systematic uncertainties. It is re-assuring that the independent analysis of RXJ1131 carried out by Birrer et al. (2015b), the one based on more flexible models carried out by Suyu et al. (2014), and the one based on ground-based adaptive optics data by Chen et al.

⁴ The original investigation by Refsdal (1964) involved the “assumption that the linear distance–redshift relation is valid”.

⁵ Importantly, the authors agreed to publish the unblinded results, no matter what.

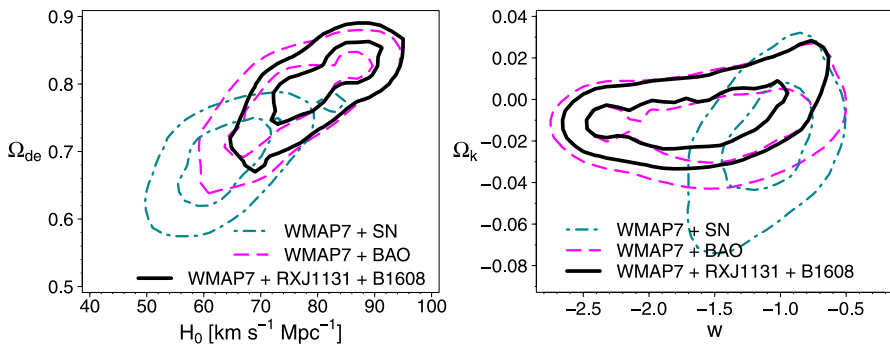


Fig. 5 Cosmological parameter constraints from time delay lenses (Suyu et al. 2013). The marginalized posterior PDFs, given the combined B1608 + 656 and RXJ1131 datasets and the assumption of an open Λ CDM cosmology with unknown dark energy equation of state, are shown in two sets of two parameter dimensions, and compared to those given contemporary BAO and Type Ia supernova data. Image reproduced with permission from Suyu et al. (2013), copyright by AAS

(2016) find results that are statistically consistent with the original blind analysis (Suyu et al. 2013).

While the sample of very well-measured lenses was being painstakingly expanded from zero to two, the exploration of statistical approaches to dealing with large samples of lenses began. Compressing the image configuration and time delay in double image systems into a single summary statistic, Oguri (2007) derived a scalable method for measuring the Hubble constant (but not the other cosmological parameters) from samples of lenses, finding $H_0 = 68 \pm 6$ (stat.) ± 8 (syst.) $\text{kms}^{-1}\text{Mpc}^{-1}$ from a sample of 16 lenses with measured time delays. The systematic uncertainties associated with this result may be hard to reduce given the approximations made: while the summary statistic is model independent, the interpretation is not.

An alternative approach is to work with more flexible lens models, fit the data for each one, and combine the whole sample in a joint inference. This is the approach taken by Saha et al. (2006), who found $72^{+8}_{-11} \text{kms}^{-1}\text{Mpc}^{-1}$ from 10 lenses (again assuming fixed curvature and dark energy parameters). The amount of information system used in this analysis was minimal: only the quasar positions and time delays were taken as inputs. The high flexibility of the free-form models employed led to a likelihood that was effectively identically 1 or 0, and thus the results are dominated by prior constraints set on the pixels and their regularization (see Coles 2008, for a description of pixel-lens in Bayesian terms). Specifically, the known physical degeneracy between density profile slope and predicted time delay (Wucknitz 2002; Suyu 2012) is broken by the choice of pixel value prior probability distribution function. This assumption was tested by Read et al. (2007), who used a hydrodynamic simulation of an elliptical galaxy to generate mock image position and time delay data, and confirm the accuracy of the previous study's Hubble constant uncertainties. With improved time delay estimates in larger samples of lenses, Paraficz and Hjorth (2010) and then Rathna Kumar et al. (2015) reduced the random uncertainty further.

While focused only on the Hubble constant and carried out unblind, and with the lens environment and line of sight mass structures remain unaccounted for and further

tests on realistic simulated galaxies warranted, these ensemble studies point the way towards a future of considerably larger sample sizes. Our aspirations towards high accuracy demand that we adopt more flexible mass models and then cope with the degeneracies; it is clear that such large-scale analysis will need careful consideration of the choice of the priors, and ideally the ability to use more information than just the image positions and time delays. We discuss these issues in detail in the next section.

6 Outlook

In this section, we discuss the future of time delay cosmography, and present a roadmap of how this measurement might be improved in the next decade. To construct the roadmap (Sect. 6.3), we will discuss in detail how to decrease the random uncertainties (increasing the precision of the method, Sect. 6.1), and the systematic uncertainties that will need to be controlled as the random uncertainties decrease (thus maintaining high accuracy, Sect. 6.2).

However, before we lay out this roadmap, we first pause and reflect on the broader context, and ask whether this is a worthy endeavor. This boils down to three simpler questions. The first question is whether time delays contain valuable information independent of other cosmological probes. As detailed in Sect. 5, the answer is a resounding yes: gravitational time delays are virtually independent of the uncertainties affecting the other established probes of dark energy, and provide valuable complementary information, chiefly on the Hubble constant, which is commonly regarded as one of the essential ingredients for interpreting other datasets such as the cosmic microwave background (Hu 2005; Suyu et al. 2012; Weinberg et al. 2013; Riess et al. 2016). We will expand on this topic in the remainder of this section by showing cosmological forecasts for gravitational time delays by themselves and in combination with other probes.

The second question is whether it is feasible to achieve an interesting level of precision and accuracy in coming years. In this mindset, interesting is defined as having total uncertainties comparable to those of other contemporary probes. This will be discussed in detail in Sects. 6.1 and 6.2 below.

The third and final question is what is the cost of pursuing this roadmap, and how this cost compares to that of other probes. Our aim is not to compute a full cost accounting, which will be almost impossible considering that each probe involves facilities, observatories, computing and brainpower, well beyond the boundaries of any individual project, collaboration, or funding agency (not to mention that the marginal cost of adding a technique to an existing program or facility is very different from what the cost of building a facility just for that purpose; for example, the cost of monitoring strongly lensed quasars in LSST data is much less than building and operating the LSST). Instead, we will aim to give an approximate sense of the observational and human resources that will be needed to pursue the roadmap.

6.1 Precision

With considerable observational and data analysis effort, the feasibility of reaching a precision of 6–7 % in time delay distance per lens has been demonstrated. The

contributions to this statistical error budget from the time delay measurement, mass model, and environment correction are at present approximately equal, and somewhat larger than the estimated systematic errors. In this situation it makes sense to enlarge the sample of lenses, to beat down the statistical uncertainties. We return to the question of how to reduce the residual systematic errors in the next section.

Coe and Moustakas (2009) made initial Fisher matrix forecasts of the likely available precision on H_0 in large future surveys. They considered several possible samples, concluding that 100 well-measured systems (with 5 % distance precision each) should provide sub-percent precision on the Hubble constant, and provide dark energy parameter constraints that are competitive with optimistic forecasts of other “Stage IV” cosmological probes. They also note that comparable constraints could be available from a sample of 4000 time delay lens systems, each with only photometric redshifts and simple image configuration model constraints (following Oguri 2007; Paraficz and Hjorth 2010). Continued investigation of both samples seems warranted, keeping in mind that the size of such a photometric sample would be set by the availability of time delays measured at the few percent level.

While Fig. 6 allows different cosmological probes to be compared (and assessed for competitiveness), it does not show the value of combining those probes. Indeed,

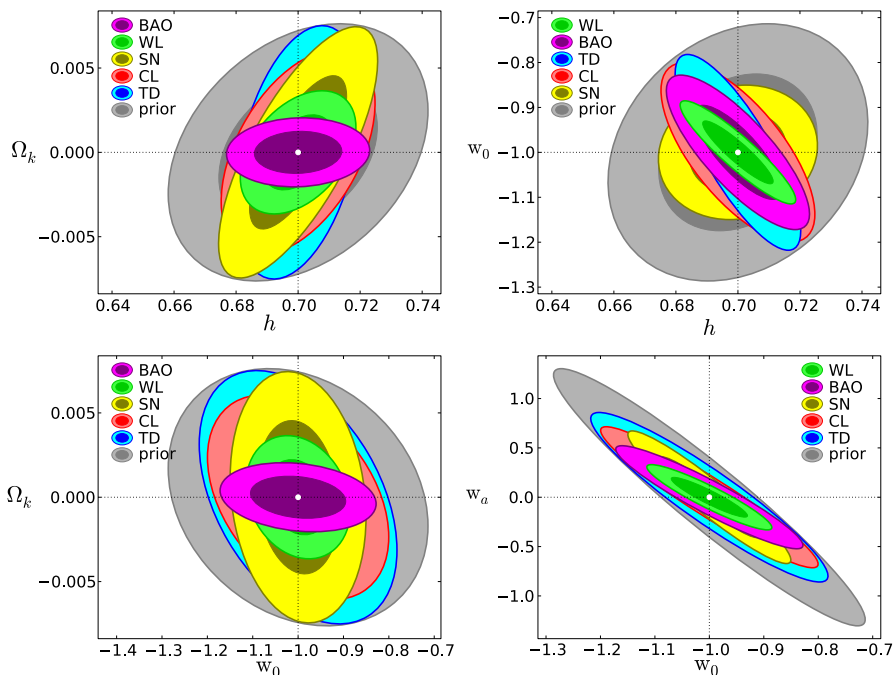


Fig. 6 Fisher matrix forecasts of cosmological parameters, based on dark energy task force assumptions and having 5 % distance precision for each of 100 time delay lenses. The stage IV cosmological probes being compared in an open CDM cosmological model with time-variable dark energy equation of state are weak lensing (WL), BAO, supernovae (SN), cluster mass function (CL) and time delay cosmography (TD). Image reproduced with permission from Coe and Moustakas (2009), copyright by AAS

Linder (2011) found that the particular combination of a type Ia supernova dataset with a time delay lens dataset holds promise, with a sample of 150 time delay distances, each measured to 5 % precision, improving the dark energy figure of merit by a factor of about 5 over what could be plausibly obtained with a sample of about 1000 Stage III supernovae and a Planck CMB prior alone.

More recently, Jee et al. (2015) have pointed out that cosmological parameter forecasts for time delay lens samples are conservative, if each lens is assumed only to measure the time delay distance. Including the angular diameter distance dependence as well can have a marked effect on the projection, especially if the spectroscopic constraints on the lens mass distribution are assumed to be very strong. The reproduction of Figure 5 from Jee et al. (2016) in the lefthand panel of Fig. 7 illustrates this. These authors find that a future sample of 55 lenses with 5 % measurements of both time delay distance and angular diameter distance would increase the figure of merit by a factor of two over that provided by a Stage III supernova, CMB, and BAO joint analysis. The righthand panel of Fig. 7 puts such improvements in the current observational context. In the B1608 + 656 analysis, the angular diameter distance dependence was accounted for during the calculation of the predicted time delay and velocity dispersion data, but the constraints on the angular diameter distance were not strong: assigning a uniform prior PDF for the cosmological parameters rather than the distances introduced degeneracy between D_d and $D_{\Delta t}$, which then seems to have been broken primarily by the time delay information to yield a 5.7 % precision prediction for $D_{\Delta t}$, and a corresponding 8.1 % precision prediction for D_d . With spatially resolved spectroscopy we should anticipate the angular diameter distance becoming more important in future analyses, with some work on simulated data needed to quantify this.

6.2 Accuracy

While the precision available from Stage III and Stage IV samples makes time delay lenses an interesting prospect for cosmology, they will, like the other probes, be limited by systematic errors. As the forecasts show, competitive contributions to joint dark energy parameter inferences correspond to sub-percent precision in characteristic distance, which implies that the residual systematic error in distance needs to be well below 1 %. This residual systematic may or may not be present at this level in every lens system—what matters is the bias in the overall measurement from the combined sample. However, the term “mean accuracy per lens” is helpful, since it reminds us that systematic errors can affect all members of a sample in the same (or at least similar) way. In this section, we revisit the primary sources of systematic error and assess the prospects for this stringent requirement to be met.

6.2.1 Time delay measurement

Liao et al. (2015) showed that a mean accuracy of 0.1 % per lens would already be achievable in plausible samples of several hundred LSST lenses, were all images to be taken in the same band. While these results are encouraging, questions about our

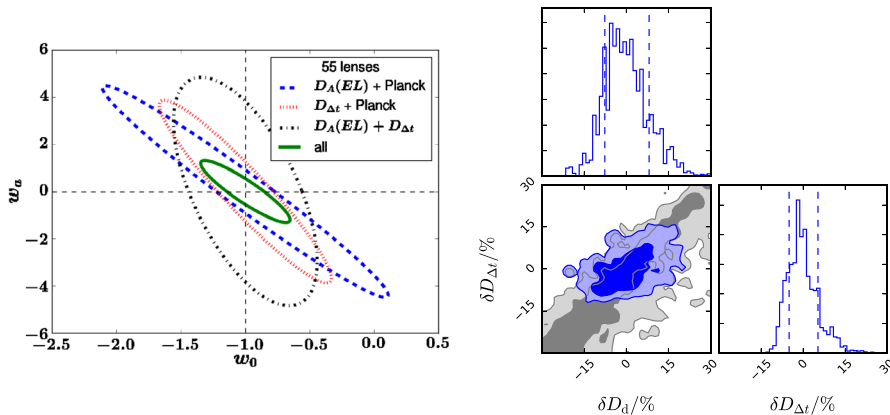


Fig. 7 Cosmological information from angular diameter distances as well as time delay distances. *Left* Fisher matrix forecasts for a future time delay lens sample where 5 % precision on each distance is assumed: the combination of distances gives a significantly more powerful constraint than the time delay distances would alone. Image reproduced with permission of IOP from [Jee et al. \(2016\)](#), copyright by SISSA. “ $D_A(EL)$ ” is the angular diameter distance to the lens from Earth. *Right* marginalized prior (gray) and posterior (blue) PDFs for the two distances in the B1608 + 656 system, assuming uninformative priors for the cosmological parameters of a flat Λ CDM model and offset and rescaled to reveal the implied percentage precisions of 5.7 and 8.1 % in $D_{\Delta t}$ and D_d , respectively (as shown by the vertical dashed lines enclosing the 68 % credible region)

ability to measure time delays from sparse, multi-filter light curves extracted from realistic images remain ([Tewes et al. 2013a](#)). Time delay measurement accuracy from LSST multi-filter light curve could be tested by a second challenge; the success of the analyses is likely to hinge on the treatment of quasar color variability (see e.g., [Schmidt et al. 2012](#); [Sun et al. 2014](#), and references therein) and chromatic microlensing (see e.g., [Hainline et al. 2013](#), and references therein). Joint inference from whole samples is likely to be important, in mitigating against both outliers and also imprecision arising from inappropriate uniform priors on population parameters. Insights into AGN physics and the stellar composition of lens galaxies would be welcome by-products of such an analysis. An alternative approach could be to continue to pursue single-filter monitoring, but at increased efficiency. Experiments with higher cadence campaigns, exploiting the short (sub-day) timescale variability of AGN are in progress ([Boroson et al. 2016](#), F. Courbin, priv. comm.).

It is worth noting that time delay perturbations, due to small-scale structure in lens plane or along line of sight, will likely not be a significant additional source of systematic error, since they primarily cause additional scatter on hour-long timescales ([Keeton and Moustakas 2009](#)).

6.2.2 Lens mass modeling

[Schneider and Sluse \(2013\)](#) have pointed out the possibility of systematic errors at the twenty percent level due to modeling assumptions (and their interaction with the mass sheet degeneracy) when fitting lensing data alone. [Suyu et al. \(2014\)](#) fitted the

same two models used by [Schneider and Sluse \(2013\)](#) to the current state-of-the-art Einstein ring imaging and lens galaxy velocity dispersion data, and found that present measurements of stellar kinematics reduce the error by a factor of 10, at least within their framework of pixelized source reconstruction. It is not clear how much of the residual 2 % uncertainty is random, and how much residual bias there is: we do not yet know how our mass modeling methods respond to the variety of lens mass distributions we expect.

An important first step has been taken by [Xu et al. \(2016\)](#), who looked at the density profiles of a sample of mock galaxies from the Illustris simulation, finding significant departures from simple power law profiles. However, they note that at the mass scales typical of galaxy-scale lenses, where the total mass density profiles happen to be well approximated by isothermal spheres ([Koopmans et al. 2009](#); [Auger et al. 2010](#)), the residual systematic uncertainty in the Hubble constant could be restricted to a few percent. Again, it remains to be verified how much of this averages out given particular, large samples of systems.

As a result of these investigations, we know that (1) the dynamical information is as important as the lensing data, (2) more complex models than simple power law density profiles will likely be needed to enable sub-percent accuracy to be reached, and (3) we now have simulated galaxies that are sufficiently realistic and suitably complex that we can carry out meaningful tests where the ground truth is very different from our assumed analysis models. The acid test will be whether we can recover the input cosmological parameters from realistic simulated high-resolution imaging and stellar spectroscopic data made using numerical simulations that resolve massive galaxies well (e.g., [Fiacconi et al. 2016](#)).

As we look ahead to samples of dozens to hundreds of lenses in the next decade, we can also consider the observational capabilities we will have in that time period. Giant segmented mirror telescopes (including the James Webb space telescope as well as planned 30 m class ground-based telescopes) will bring up to a factor of 10 increase in angular resolution beyond what HST and today's 10-m class adaptive optics-enabled telescopes can deliver, improving further the available Einstein ring constraints. These facilities will be instrumented with integral field unit spectrographs that will provide spatially resolved spectroscopy of the lens galaxy stellar populations. It is yet to be seen how accurately lens mass distributions can be modeled with such data: extending the realistic lens galaxy data simulation work to include them would seem to be very important. The "crash test" of [Barnabè et al. \(2009\)](#) was an excellent start in this direction, probing as it did the performance of a fully self-consistent lensing and dynamics modeling code on a numerically simulated lens galaxy mock dataset.

The upcoming increase in available precision per lens will support significantly more flexible mass models, as reviewed in Sect. 4.2. The opportunity here is to find a flexible mass model whose parameters can be taken to have been drawn from a relatively simple prior PDF, which could be derived from either large samples of observed non-lens galaxies, plausible hydrodynamic simulated galaxies, or both.

The mass sheet degeneracy, and indeed all model parameter degeneracies are broken by incorporating more information, but this needs to be done in such a way as to

not introduce bias. Using flexible mass models with reasonably broad but not uninformative priors is the first step, but unless these priors are themselves movable, the introduced bias might remain. The clear-cut solution is to learn the hyper-parameters that govern the intrinsic distribution of mass model parameters from the data as well. It is really the prior on these “hyper-parameters” that needs to come from simulations. An initial attempt at this kind of “hierarchical inference” can be found in the analysis of [Sonnenfeld et al. \(2015\)](#), where the authors infer the values of some 28 hyper-parameters assumed to govern the scaling relations between massive galaxies, as well as the selection function of the lens sample. As surveys yield larger and larger samples of lenses, joint inferences from ensembles of all lenses (time delay and otherwise) will bring in more information about the density structure of somewhat self-similar massive galaxies.

In addition to carrying out tests on simulated data, it is important to continue empirical investigations of systematic errors. In addition to the generally applicable strategy of comparing the cosmological parameter estimates between individual systems or subsets of systems to measure whether statistical uncertainties are underestimated, we must continue to look for other independent tests. An interesting example is that of the multiply imaged supernova “Refsdal”. Several teams carried out modeling analyses of this lens system, to predict in a truly blind fashion the magnification, timing, and position of the next appearance of the supernova ([Kelly et al. 2015](#); [Oguri 2015](#); [Sharon and Johnson 2015](#); [Jauzac et al. 2016](#); [Treu et al. 2016](#); [Kawamata et al. 2016](#); [Grillo et al. 2016](#); [Diego et al. 2016](#)). Even though the deflector is a merging cluster, and thus significantly more challenging to model than the typical relaxed elliptical galaxies used in time delay cosmography, several teams managed to predict the event ([Treu et al. 2016](#); [Kelly et al. 2016](#)) within the estimated model prediction uncertainties. It is particularly re-assuring that the code GLEE ([Suyu and Halkola 2010](#)), which was designed and used extensively to model time delay lenses for cosmography ([Suyu et al. 2010, 2013, 2014](#)), performed very well ([Grillo et al. 2016](#); [Kelly et al. 2016](#)), along with other methods based on similar assumptions ([Kawamata et al. 2016](#)). As the precision of time delay cosmography increases with sample size it will be important to seize any new opportunity to carry out additional blind tests, e.g., by predicting time delays of lens quasars before measuring them, and by actively searching for multiply imaged supernovae in galaxy-scale lenses ([Oguri and Marshall 2010](#); [Quimby et al. 2014](#)). Lensed supernovae, especially if they are type Ia, would be particularly important if they provide a direct measurement of magnification ([Patel et al. 2014](#); [Nordin et al. 2014](#); [Rodney et al. 2015](#)) as well as time delay and thus a way to break the mass sheet degeneracy.

6.2.3 Environment and line of sight characterization

The current methodology (Sect. 4.3) includes dependencies on both cosmological simulations and reference imaging surveys. The Stage III and IV wide field surveys will help with the latter, providing much larger, more homogeneous sets of control fields. Systematic errors associated with calibrating against simulations is the bigger problem, and both the number counts and 3D reconstruction approaches that have been implemented to date are affected. [Collett et al. \(2013\)](#) give some indication of

the magnitude of the issue, finding a bias of 3 % in the average inferred time delay distance when assuming a stellar mass to halo mass relation that is incorrect but still consistent with other observations. This reduces to 1–2 % if the bright galaxies in the lens fields have spectroscopic redshifts, suggesting that this kind of data will continue to be important.

The 3D reconstruction approach can, in principle, be made to be independent from simulations (indeed, this was a design feature of [McCully et al. 2014](#)). However, more information about mass in the Universe will be required. Both [McCully et al. \(2014\)](#) and [Collett et al. \(2013\)](#) use halo models, with very simplistic treatments of the mass outside of halos, and the voids between them. Both weak shear data and clustering information could be used to improve the accuracy of these models; statistical halo models are already well constrained by summary statistics from these probes (e.g., [Coupon et al. 2015](#)), and these results are already potentially useful (although the scatter in the model's relations will likely need to be taken into account). Covariance with cosmic shear, galaxy clustering, and the halo mass function may then have to be accounted for in any joint cosmological parameter inferences; this may turn out to be negligible, once quantified. Some mitigation of the environment and line of sight systematics could be achieved by selecting low-density lines of sight ([Collett et al. 2013](#)), but this selection would have to be done with some care, propagating all the uncertainties.

A key point made by [McCully et al. \(2014, 2016\)](#) is that the mass structures external to the primary lens should, in principle, be included in the lens model itself. Doing this would allow the correct multiple lens plane formalism to be employed, thereby reducing the systematic error introduced by the single lens plane approximation. This approach is being actively pursued in the ongoing analyses (K. Wong, priv. comm.). An interesting feature of multiple plane lensing is that the appearance of the lens galaxy is also affected by weak lensing due to foreground mass structures: this may well need to be taken into account when striving for high-accuracy modeling of the primary lens (R. Blandford and S. Birrer, priv. comm.).

Even when all the above systematics have been investigated and tested for, others that are unforeseen may remain. Strategies for detecting these “unknown unknowns” include jack-knife testing, which will become possible with larger samples. Other kinds of “null tests” may also be possible when we are out of the small number statistics regime: research is needed on developing such tests. The ultimate test is cosmological parameter consistency with other datasets, but for this comparison to be meaningful the analysis of each dataset must be done blindly, to avoid unconscious experimenter bias and the resulting groupthink towards (or away from) concordance (see e.g., [Conley et al. 2006](#); [Suyu et al. 2013](#)). In principle, all systematics tests need to be done before unblinding; as a result, end to end tests on highly realistic mock data will become ever more important. The time delay challenge was carried out blind; similarly designed lens modeling and environment characterization challenges are called for too. Success at blind cosmological parameter recovery from realistic mock samples is the surest way to generate confidence in a probe's accuracy.

6.3 Roadmap

We conclude the outlook section by proposing an ambitious, yet (in our opinion) feasible roadmap for time delay cosmography in the next decade. This roadmap aims to achieve $\sim 0.5\%$ precision on time delay distance⁶ by 2027 (by which time the 5-year LSST light curves should be in hand), building on the tools and techniques demonstrated in the past 15 years and exploiting the large-scale surveys that are currently under way or planned. It is based on a specific strategy, consisting of constructing the most precise and accurate models of each lens based on rich datasets for each system (alternative strategies are discussed at the end of this section). Specifically, for each system one needs the following:

1. Time delays precise to better than 3 %;
2. High-resolution imaging (resolution much better than the Einstein radius) with point spread function known well enough to reconstruct the differences in Fermat potential to better than 3 % precision;
3. Spectroscopic redshifts of the deflector and the source;
4. Stellar velocity dispersion of the deflector to better than 10 % precision, possibly spatially resolved;
5. Imaging and spectroscopic data sufficient to characterize the weak lensing effects due to structure along the line of sight to better than 3 % precision.

These targets can be met with present technology, as it has already been demonstrated for a few systems (Tewes et al. 2013b; Suyu et al. 2013), and the observational requirements have been investigated for a variety of telescopes and configurations (Greene et al. 2013; Collett et al. 2013; Meng et al. 2015; Linder 2015).

The proposed roadmap is summarized in Fig. 8. The shaded region represents an estimate of the ensemble precision attainable on $D_{\Delta t}$,⁷ ranging from the most conservative to the most favorable scenario. The most conservative case assumes only a central velocity dispersion measurement for each system, while the most favorable scenario involves spatially resolved stellar velocity dispersions, obtained either from space or from the ground assisted by adaptive optics (Agnello et al. in prep.). We neglect the additional independent information that in principle can be obtained via the angular diameter distance dependence (Jee et al. 2016). As discussed in Sect. 6.1, this additional piece of information would in principle improve the constraints on cosmological parameters from time delay lenses, so this envelope should be regarded as a conservative estimate.

The roadmap is divided into steps, whose timing is dictated by available observational facilities. The first step in the roadmap is the analysis of two systems that

⁶ For simplicity, we refer to equivalent uncertainty on an average time delay distance at the typical redshift of the deflector and source. In practice of course, there will be a distribution of redshifts and thus of individual distances. As the way in which the time delay distance depends on cosmological parameters varies slightly with redshift, the analysis of a real sample of lenses will have the added benefit of breaking some of the degeneracies between the cosmological parameters, and reducing the uncertainties more rapidly than if all the systems were at the same redshift.

⁷ The time delay distance referred to here is the same as ensemble average quantity that Coe and Moustakas (2009) call τ_C .

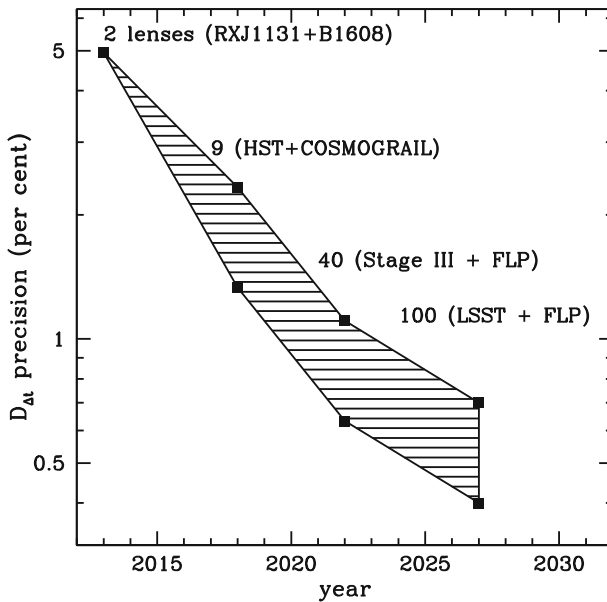


Fig. 8 Roadmap for time delay cosmography. The *shaded region* represents the estimated range of uncertainty attainable on the effective (ensemble) time delay distance $D_{\Delta t}$ as a function of time, over the next 10 years. Points on the roadmap are labeled by the types of survey and follow-up (FLP) observation required

was published in 2013, and was based on COSMOGRAIL time delays, HST imaging, Keck spectroscopy, and other ancillary data from a variety of sources.

The second step consists of the full analysis of nine lens systems for which time delays have been measured by the COSMOGRAIL team, and for which HST imaging is being completed this year (HST-GO-14254; PI: Treu). Completing the second step by the launch of the James Webb space telescope at the end of 2018, and in doing so delivering $\sim 2\%$ distance precision, would be ideal, so as to provide a useful comparison for expected improvements in local distance ladder measurements.

The third step will require the discovery of new lenses, in addition to the usual follow-up (FLP) effort. Systematic searches are currently under way based on large-scale surveys such as the Dark Energy Survey or Hyper Suprime-Camera Survey (Agnello et al. 2015; More et al. 2016), and should discover hundreds of new lensed quasar systems by the end of the decade (Oguri and Marshall 2010), while providing high-quality photometric lens environment information from the survey itself. Focused follow-up of a carefully selected sample of systems should be sufficient to reach the goal for step 3, that is, $\sim 1\%$ distance precision from 40 lenses in 5 years (i.e., by 2022). The selected sample should consist of as many quads as possible, since they contain more cosmological information and favor systems with time delays in the range 50–150 days, such that they are measurable at the $< 3\%$ level in one observing season with daily cadence. It is worth noting that in the high-quality follow-up approach each individual system provides a highly informative measurement of cosmology and, therefore, this method is very robust with respect to the precise selection function

imposed by the search and monitoring algorithms (Collett and Cunningham 2016), at the level of accuracy required in this step. The observational bottle necks are likely going to be the time delay measurements, which will require dedicated monitoring on 1–4 m class telescopes, and high-resolution imaging (Treu et al. 2013).

Scaling up to the fourth step will require a change of strategy, to cope with the intrinsically fainter targets and larger sample size. One natural strategy will consist of using time delays measured from LSST light curves (Liao et al. 2015), perhaps supplemented in part from 1–4 m telescopes to increase the cadence, or potentially from a dedicated lens monitoring satellite (Moustakas et al. 2008). Unfortunately, LSST imaging will be insufficient for detailed modeling, and higher resolution imaging will be required (Meng et al. 2015). Planned surveys like Euclid and WFIRST will be excellent at discovering new lenses, but probably will have insufficient depth and resolution except for the brightest systems. Therefore, targeted follow-up will be required, achievable either with JWST from space, or with improved adaptive optics systems on 8–10 m class ground-based telescopes (Marshall 2007; Chen et al. 2016; Rusu et al. 2016). Integral field spectrographs on giant segmented mirror telescopes will be the ideal complement to LSST, by providing the necessary high-resolution imaging and spectroscopy with relatively short exposure times (e.g., Skidmore 2015). Much of the information needed for lens environment characterization will again come from the surveys themselves, although synergy with spectroscopic surveys should be explored to increase the redshift accuracy. This fourth step aims to reach $\sim 0.5\%$ precision, through follow-up of systems discovered and monitored in the first five years of the LSST survey.

Converting the uncertainty in time delay distance $D_{\Delta t}$ to cosmological parameters requires specific assumptions about the cosmological model and priors from independent measurements. For step 1, the equivalent precision on H_0 using WMAP7 prior in one parameter extensions of Λ CDM is 4–5 %. The forecast for step 2 with WMAP9 and Planck priors is shown in Fig. 9. For steps 3 and 4, the equivalent precision on H_0 is in the range 1.1–1.3 % and 0.8–1.0 % respectively, assuming “Planck + Stage II” priors (Coe and Moustakas 2009).

In addition to the observational challenges, the main challenge in pursuing this roadmap is likely to be the analysis cost. Lens modeling is at present fairly labor intensive, requiring several months of work per system by an expert modeler. This high labor cost is chiefly due to code development. Up to now, the analysis of each single lens has required the development and testing of new features (e.g., multi-plane lensing, point spread function reconstruction; Suyu et al. 2016, in prep.). To analyze the future large samples, the analysis codes will have to transition from development to production, reducing substantially the investigator time per system. Distributing the work among a large team of modelers will likely be necessary to speed things up and keep modeling uncertainties in check.

Naturally, this proposed roadmap is not the only possible way forward. As discussed earlier in this section, several authors have proposed the analysis of larger samples of lenses, each with fewer ancillary data and thus lower precision per system. Alternatively, one could imagine a hybrid strategy in which a subset of the lenses are analyzed in great detail with lots of ancillary data, and the lessons learned from that subset are propagated to a large sample through judicious use of priors.

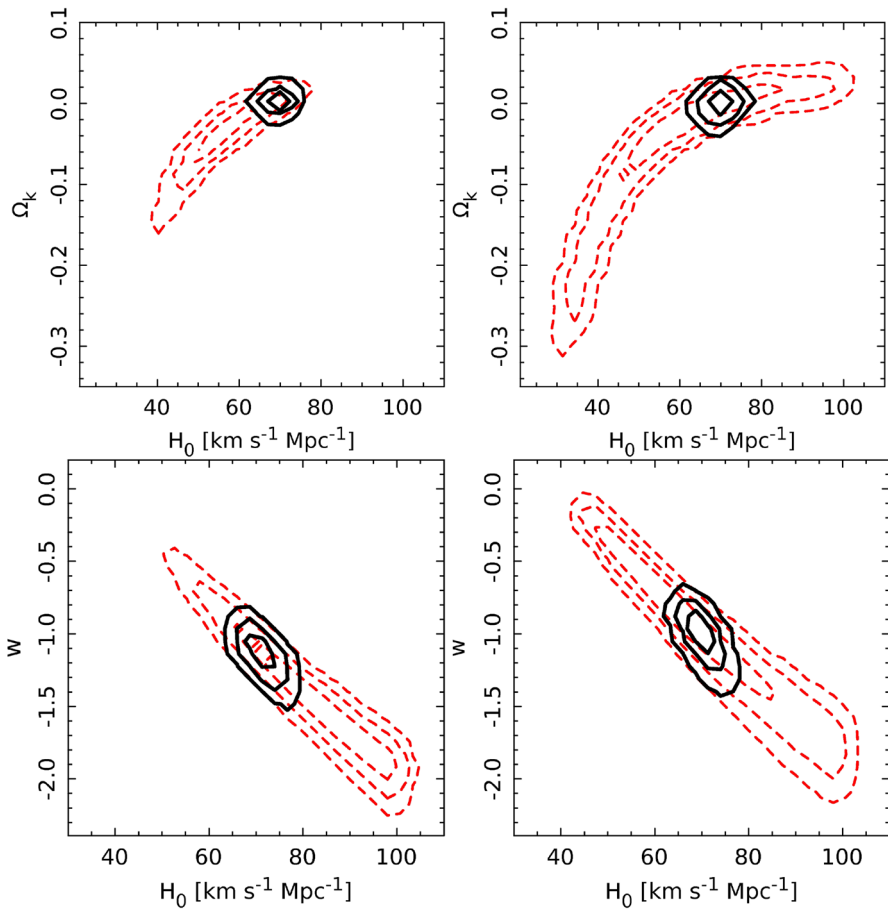


Fig. 9 Cosmological forecast (black solid lines represent the 68, 95, and 99 % posterior probability contours) for step 2 in the roadmap (see Fig. 8 and Sect. 6.3 for details), assuming one parameter extensions of flat Λ CDM, and Planck (left column) and WMAP9 (right column) priors (red dashed lines). Figure courtesy of S.H. Suyu

7 Summary

We reviewed gravitational time delays as a tool for measuring cosmological parameters. In addition to giving a brief introduction to the theoretical underpinnings of the method, we discussed the past history of the field, before turning to present-day accomplishments and the challenges ahead. The main points of this review can be summarized as follows:

1. From a theoretical point of view gravitational time delays are a clean and well-understood probe of cosmic acceleration. Conceptually, each time delay measurement provides a one-step measurement of absolute distance. The typical redshifts of deflectors and sources span the range between $z \sim 2$ and today, covering the era of cosmic time during which dark energy rose to prominence.

2. Even though the potential cosmological application of strongly lensed, time-variable sources was recognized as early as 1964, it took decades for the method to come to practical fruition. Two sets of challenges have been overcome over the past 15 years. Observationally, the main challenge has been organizing long-term monitoring campaigns and mustering the range of resources required to constrain accurate mass models. Theoretically, the main challenge consisted of learning how to exploit the available information to construct lens models with realistic estimates of the uncertainties.
3. It has been demonstrated through blind measurements that each individual system can deliver a measurement of absolute distance to about 6–7 % total uncertainty, given current data quality. The power of the method is currently limited by the number of systems with well-measured time delays and sufficient ancillary data to carry out detailed modeling ($\lesssim 10$ at the time of writing).
4. Systematic searches for strongly lensed quasars are under way and should be able to increase the cosmographic sample size by more than an order of magnitude in the next decade. With improvements in follow-up image resolution and spatially resolved spectroscopy as well, we can aspire to sub-percent precision in the Hubble constant by the middle of the next decade.
5. Before LSST, dedicated monitoring campaigns will be required to measure each time delay; LSST can potentially alter the landscape, if it can deliver hundreds of time delays from the survey data themselves.
6. Throughout the next decade to deliver the available precision it will be necessary to obtain a small amount of high-quality follow-up data to minimize the uncertainty per system. These include: high-resolution imaging from space or with adaptive optics; redshifts; stellar velocity dispersions, and spatially resolved kinematics of the deflectors. These data can be obtained from the James Webb Space Telescope or large and extremely large ground-based telescopes with adaptive optics.
7. As samples increase, further work will be needed to understand, quantify and mitigate against potential systematic errors in the method. Extensive parameter recovery tests on realistic simulated monitoring, high-resolution imaging, spatially resolved spectroscopy, and field weak lensing and photometry will be essential to ensure that systematic errors are kept sub-dominant, the precision of the method is realized, and an accurate cosmological measurement is achieved.

In gravitational time delays we have a theoretically sound, experimentally competitive, and cost-effective cosmographic tool. Like for every other probe, a lot of hard work will be necessary to reach the sub-percent level of precision and accuracy that is needed to make progress. This effort seems well motivated, not only by the ultimate goal of improving our understanding of the fundamental constituents of the universe, but also by the opportunity to use lensed quasars to learn about the astrophysics of dark matter (Metcalf and Madau 2001; Dalal and Kochanek 2002; Metcalf 2005; Xu et al. 2009; Vegetti et al. 2014; Nierenberg et al. 2014), active galactic nuclei (Poindexter et al. 2008; Eigenbrod et al. 2008a, b; Blackburne et al. 2010; MacLeod 2015), and stars (Schechter et al. 2014).

Acknowledgements We are grateful to S. Suyu and E. Komatsu for insightful discussions about the cosmological distance information content of time delay lenses, and to S. Suyu for making the B1608 +

656 MCMC chains available for us to make Fig. 7. We thank A. Agnello, M. Bartelmann, S. Birrer, V. Bonvin, D. Coe, T. Collett, F. Courbin, I. Jee, C. Kochanek, E. Linder, D. Sluse, S. Suyu, and M. Tewes for very valuable feedback on a draft of this review. T.T. thanks the Packard Foundation for generous support through a Packard Research Fellowship, the NSF for funding through NSF Grant AST-1450141, “Collaborative Research: Accurate cosmology with strong gravitational lens time delays”. P.J.M. acknowledges support from the U.S. Department of Energy under Contract Number DE-AC02-76SF00515.

References

- Aghamousa A, Shafieloo A (2015) Fast and reliable time delay estimation of strong lens systems using the smoothing and cross-correlation methods. *ApJ* 804:39. doi:[10.1088/0004-637X/804/1/39](https://doi.org/10.1088/0004-637X/804/1/39). arXiv:[1410.8122](https://arxiv.org/abs/1410.8122)
- Agnello A, Treu T, Ostrovski F, Schechter PL, Buckley-Geer EJ, Lin H, Auger MW, Courbin F, Fassnacht CD, Frieman J, Kuropatkin N, Marshall PJ, McMahon RG, Meylan G, More A, Suyu SH, Rusu CE, Finley D, Abbott T, Abdalla FB, Allam S, Annis J, Banerji M, Benoit-Lévy A, Bertin E, Brooks D, Burke DL, Rosell AC, Kind MC, Carretero J, Cunha CE, D’Andrea CB, da Costa LN, Desai S, Diehl HT, Dietrich JP, Doel P, Eifler TF, Estrada J, Neto AF, Flaughner B, Fosalba P, Gerdes DW, Gruen D, Gutierrez G, Honscheid K, James DJ, Kuehn K, Lahav O, Lima M, Maia MAG, March M, Marshall JL, Martini P, Melchior P, Miller CJ, Miquel R, Nichol RC, Ogando R, Plazas AA, Reil K, Romer AK, Roodman A, Sako M, Sanchez E, Santiago B, Scarpine V, Schubnell M, Sevilla-Noarbe I, Smith RC, Soares-Santos M, Sobreira F, Suchyta E, Swanson MEC, Tarle G, Thaler J, Tucker D, Walker AR, Wechsler RH, Zhang Y (2015) Discovery of two gravitationally lensed quasars in the dark energy survey. *MNRAS* 454:1260–1265. doi:[10.1093/mnras/stv2171](https://doi.org/10.1093/mnras/stv2171). arXiv:[1508.01203](https://arxiv.org/abs/1508.01203)
- Auger MW, Fassnacht CD, Abrahamse AL, Lubin LM, Squires GK (2007) The gravitational lens-galaxy group connection. II. Groups associated with B2319+051 and B1600+434. *AJ* 134:668–679. doi:[10.1086/519238](https://doi.org/10.1086/519238). arXiv:[astro-ph/0603448](https://arxiv.org/abs/astro-ph/0603448)
- Auger MW, Treu T, Bolton AS, Gavazzi R, Koopmans LVE, Marshall PJ, Moustakas LA, Burles S (2010) The sloan lens ACS survey. X. Stellar, dynamical, and total mass correlations of massive early-type galaxies. *ApJ* 724:511–525. doi:[10.1088/0004-637X/724/1/511](https://doi.org/10.1088/0004-637X/724/1/511). arXiv:[1007.2880](https://arxiv.org/abs/1007.2880)
- Bar-Kana R (1996) Effect of large-scale structure on multiply imaged sources. *ApJ* 468:17. doi:[10.1086/177666](https://doi.org/10.1086/177666). arXiv:[astro-ph/9511056](https://arxiv.org/abs/astro-ph/9511056)
- Barnabè M, Nipoti C, Koopmans LVE, Vegetti S, Ciotti L (2009) Crash-testing the CAULDRON code for joint lens and dynamics analysis of early-type galaxies. *MNRAS* 393:1114–1126. doi:[10.1111/j.1365-2966.2008.14208.x](https://doi.org/10.1111/j.1365-2966.2008.14208.x). arXiv:[0808.3916](https://arxiv.org/abs/0808.3916)
- Bartelmann M (2010) Topical review gravitational lensing. *Class Quant Grav* 27(23):233001. doi:[10.1088/0264-9381/27/23/233001](https://doi.org/10.1088/0264-9381/27/23/233001). arXiv:[1010.3829](https://arxiv.org/abs/1010.3829)
- Bennett CL, Larson D, Weiland JL, Jarosik N, Hinshaw G, Odegard N, Smith KM, Hill RS, Gold B, Halpern M, Komatsu E, Nolte MR, Page L, Spergel DN, Wollack E, Dunkley J, Kogut A, Limon M, Meyer SS, Tucker GS, Wright EL (2013) Nine-year wilkinson microwave anisotropy probe (WMAP) observations: final maps and results. *ApJs* 208:20. doi:[10.1088/0067-0049/208/2/20](https://doi.org/10.1088/0067-0049/208/2/20). arXiv:[1212.5225](https://arxiv.org/abs/1212.5225)
- Birrer S, Amara A, Refregier A (2015) Gravitational lens modeling with basis sets. *ApJ* 813:102. doi:[10.1088/0004-637X/813/2/102](https://doi.org/10.1088/0004-637X/813/2/102). arXiv:[1504.07629](https://arxiv.org/abs/1504.07629)
- Birrer S, Amara A, Refregier A (2015) The mass-sheet degeneracy and time-delay cosmography: analysis of the strong lens RXJ1131-1231. *JCAP*. arXiv:[1511.03662](https://arxiv.org/abs/1511.03662) (submitted)
- Blackburne JA, Pooley D, Rappaport S, Schechter PL (2010) Sizes and temperature profiles of quasar accretion disks from chromatic microlensing. arXiv:[1007.1665v1](https://arxiv.org/abs/1007.1665v1) [astro-ph.CO]
- Blandford RD, Narayan R (1992) Cosmological applications of gravitational. *ARA A* 30:311–358. doi:[10.1146/annurev.aa.30.090192.001523](https://doi.org/10.1146/annurev.aa.30.090192.001523)
- Bonvin V, Tewes M, Courbin F, Kuntzer T, Sluse D, Meylan G (2016) COSMOGRAIL: the COSmological MONitoring of GRAVItational Lenses. XV. Assessing the achievability and precision of time-delay measurements. *A A* 585:A88. doi:[10.1051/0004-6361/201526704](https://doi.org/10.1051/0004-6361/201526704). arXiv:[1506.07524](https://arxiv.org/abs/1506.07524)
- Borison TA, Moustakas LA, Romero-Wolf A, McCully C (2016) Using the LCOGT network to measure a high-precision time delay in the four-image gravitational lens HE0435-1223. In: American Astronomical Society Meeting Abstracts, vol 227, p 338.04
- Brewer BJ, Lewis GF (2006) The Einstein ring 0047–2808 revisited: a Bayesian inversion. *ApJ* 651:8–13. doi:[10.1086/507475](https://doi.org/10.1086/507475). arXiv:[astro-ph/0606714](https://arxiv.org/abs/astro-ph/0606714)

- Browne IWA et al (2003) The cosmic lens all-sky survey—II. Gravitational lens candidate selection and follow-up. *MNRAS* 341:13–32. doi:[10.1046/j.1365-8711.2003.06257.x](https://doi.org/10.1046/j.1365-8711.2003.06257.x). [arXiv:astro-ph/0211069](https://arxiv.org/abs/astro-ph/0211069)
- Burud I, Courbin F, Magain P, Lidman C, Hutsemékers D, Kneib JP, Hjorth J, Brewer J, Pompei E, Germany L, Pritchard J, Jaunsen AO, Letawe G, Meylan G (2002) An optical time-delay for the lensed BAL quasar HE 2149–2745. *A A* 383:71–81. doi:[10.1051/0004-6361:20011731](https://doi.org/10.1051/0004-6361:20011731). [arXiv:astro-ph/0112225](https://arxiv.org/abs/astro-ph/0112225)
- Chen GCF, Suyu SH, Wong KC, Fassnacht CD, Chiueh T, Halkola A, Hu I, Auger MW, Koopmans LVE, Lagattuta DJ, McKean JP, Vegetti S (2016) SHARP—III: first use of adaptive optics imaging to constrain cosmology with gravitational lens time delays. [arXiv:1601.01321](https://arxiv.org/abs/1601.01321)
- Coe D, Moustakas LA (2009) Cosmological constraints from gravitational lens time delays. *ApJ* 706:45–59. doi:[10.1088/0004-637X/706/1/45](https://doi.org/10.1088/0004-637X/706/1/45). [arXiv:0906.4108](https://arxiv.org/abs/0906.4108)
- Coles J (2008) A new estimate of the hubble time with improved modeling of gravitational lenses. *ApJ* 679:17–24. doi:[10.1086/587635](https://doi.org/10.1086/587635). [arXiv:0802.3219](https://arxiv.org/abs/0802.3219)
- Collett TE, Cunningham S (2016) Selection biases in time-delay cosmography. *Mon Not R Astron Soc* (submitted). [arXiv:1605.08341](https://arxiv.org/abs/1605.08341)
- Collett TE, Marshall PJ, Auger MW, Hilbert S, Suyu SH, Greene Z, Treu T, Fassnacht CD, Koopmans LVE, Bradač M, Blandford RD (2013) Reconstructing the lensing mass in the universe from photometric catalogue data. *Mon Not R Astron Soc* 432:679. doi:[10.1093/mnras/stt504](https://doi.org/10.1093/mnras/stt504)
- Conley A, Goldhaber G, Wang L, Aldering G, Amanullah R, Commings ED, Fadeyev V, Folatelli G, Garavini G, Gibbons R, Goobar A, Groom DE, Hook I, Howell DA, Kim AG, Knop RA, Kowalski M, Kuznetsova N, Lidman C, Nobili S, Nugent PE, Pain R, Perlmutter S, Smith E, Spadafora AL, Stanishev V, Strovink M, Thomas RC, Wood-Vasey WM, Supernova Cosmology Project (2006) Measurement of Ω_m , Ω from a blind analysis of type Ia supernovae with CMAGIC: using color information to verify the acceleration of the universe. *ApJ* 644:1–20. doi:[10.1086/503533](https://doi.org/10.1086/503533). [arXiv:astro-ph/0602411](https://arxiv.org/abs/astro-ph/0602411)
- Coupon J, Arnouts S, van Waerbeke L, Moutard T, Ilbert O, van Uitert E, Erben T, Garilli B, Guzzo L, Heymans C, Hildebrandt H, Hoekstra H, Kilbinger M, Kitching T, Mellier Y, Miller L, Scodeggio M, Bonnett C, Branchini E, Davidzon I, De Lucia G, Fritz A, Fu L, Hudelot P, Hudson MJ, Kuijken K, Leauthaud A, Le Fèvre O, McCracken HJ, Moscardini L, Rowe BTP, Schrabback T, Semboloni E, Velander M (2015) The galaxy-halo connection from a joint lensing, clustering and abundance analysis in the CFHTLenS/VIPERS field. *MNRAS* 449:1352–1379. doi:[10.1093/mnras/stv276](https://doi.org/10.1093/mnras/stv276). [arXiv:1502.02867](https://arxiv.org/abs/1502.02867)
- Courbin F, Magain P, Keeton CR, Kochanek CS, Vanderriest C, Jaunsen AO, Hjorth J (1997) The geometry of the quadruply imaged quasar PG 1115+080: implications for H_0 . *A A* 324:L1–L4 [astro-ph/9705093](https://arxiv.org/abs/astro-ph/9705093)
- Courbin F, Saha P, Schechter PL (2002) Quasar lensing. In: Courbin F, Minniti D (eds) *Gravitational lensing: an astrophysical tool*, Lecture notes in physics, vol 608. Springer Verlag, Berlin, p 1. [arXiv:astro-ph/0208043](https://arxiv.org/abs/astro-ph/0208043)
- Courbin F, Eigenbrod A, Vuissoz C, Meylan G, Magain P (2005) COSMOGRAIL: the COSmological MONitoring of GRAvitational Lenses. In: Mellier Y, Meylan G (eds) *Gravitational lensing impact on cosmology*, IAU Symposium, vol 225, pp 297–303. doi:[10.1017/S1743921305002097](https://doi.org/10.1017/S1743921305002097)
- Courbin F, Chantry V, Revaz Y, Sluse D, Faure C, Tewes M, Eulaers E, Koleva M, Asfandiyarov I, Dye S, Magain P, van Winckel H, Coles J, Saha P, Ibrahimov M, Meylan G (2011) COSMOGRAIL: the COSmological MONitoring of GRAvitational Lenses. IX. Time delays, lens dynamics and baryonic fraction in HE 0435–1223. *A A* 536:A53. doi:[10.1051/0004-6361/201015709](https://doi.org/10.1051/0004-6361/201015709). [arXiv:1009.1473](https://arxiv.org/abs/1009.1473)
- Courteau S, Cappellari M, de Jong RS, Dutton AA, Emsellem E, Hoekstra H, Koopmans LVE, Mamon GA, Maraston C, Treu T, Widrow LM (2014) Galaxy masses. *Rev Mod Phys* 86:47–119. doi:[10.1103/RevModPhys.86.47](https://doi.org/10.1103/RevModPhys.86.47). [arXiv:1309.3276](https://arxiv.org/abs/1309.3276)
- Dahle H, Gladders MD, Sharon K, Bayliss MB, Rigby JR (2015) Time delay measurements for the cluster-lensed sextuple quasar SDSS J2222+2745. *ApJ* 813:67. doi:[10.1088/0004-637X/813/1/67](https://doi.org/10.1088/0004-637X/813/1/67). [arXiv:1505.06187](https://arxiv.org/abs/1505.06187)
- Dalal N, Kochanek CS (2002) Direct detection of cold dark matter substructure. *ApJ* 572:25–33. doi:[10.1086/340303](https://doi.org/10.1086/340303). [arXiv:astro-ph/0111456](https://arxiv.org/abs/astro-ph/0111456)
- Diego JM, Broadhurst T, Chen C, Lim J, Zitrin A, Chan B, Coe D, Ford HC, Lam D, Zheng W (2016) A free-form prediction for the reappearance of supernova Refsdal in the Hubble frontier fields cluster MACSJ1149.5+2223. *MNRAS* 456:356–365. doi:[10.1093/mnras/stv2638](https://doi.org/10.1093/mnras/stv2638). [arXiv:1504.05953](https://arxiv.org/abs/1504.05953)
- Dobler G, Fassnacht CD, Treu T, Marshall P, Liao K, Hojjati A, Linder E, Rumbaugh N (2015) Strong lens time delay challenge. I. Experimental design. *ApJ* 799:168. doi:[10.1088/0004-637X/799/2/168](https://doi.org/10.1088/0004-637X/799/2/168)
- Efstathiou G (2014) H_0 revisited. *MNRAS* 440:1138–1152. doi:[10.1093/mnras/stu278](https://doi.org/10.1093/mnras/stu278). [arXiv:1311.3461](https://arxiv.org/abs/1311.3461)

- Eigenbrod A, Courbin F, Vuissoz C, Meylan G, Saha P, Dye S (2005) COSMOGRAIL: The COSmological MONitoring of GRAVItational Lenses. I. How to sample the light curves of gravitationally lensed quasars to measure accurate time delays. *A A* 436:25–35. doi:[10.1051/0004-6361:20042422](https://doi.org/10.1051/0004-6361:20042422). [arXiv:astro-ph/0503019](https://arxiv.org/abs/astro-ph/0503019)
- Eigenbrod A, Courbin F, Meylan G, Agol E, Anguita T, Schmidt RW, Wambsganss J (2008a) Microlensing variability in the gravitationally lensed quasar QSO 2237+0305 \equiv the Einstein cross. II. Energy profile of the accretion disk. *A A* 490:933–943. doi:[10.1051/0004-6361:200810729](https://doi.org/10.1051/0004-6361:200810729). [arXiv:0810.0011](https://arxiv.org/abs/0810.0011)
- Eigenbrod A, Courbin F, Sluse D, Meylan G, Agol E (2008b) Microlensing variability in the gravitationally lensed quasar QSO 2237+0305 \equiv the Einstein Cross. I. Spectrophotometric monitoring with the VLT. *A A* 480:647–661. doi:[10.1051/0004-6361:20078703](https://doi.org/10.1051/0004-6361:20078703). [arXiv:0709.2828](https://arxiv.org/abs/0709.2828)
- Ellis RS (2010) Gravitational lensing: a unique probe of dark matter and dark energy. *Philos Trans R Soc Lond Ser A* 368:967–987. doi:[10.1098/rsta.2009.0209](https://doi.org/10.1098/rsta.2009.0209)
- Eulaers E, Tewes M, Magain P, Courbin F, Asfandiyarov I, Ehgamberdiev S, Rathna Kumar S, Stalín CS, Prabhu TP, Meylan G, Van Winckel H (2013) COSMOGRAIL: the COSmological MONitoring of GRAVItational Lenses XII Time delays of the doubly lensed quasars SDSS J1206+4332 and HS 2209+1914. *A A* 553:A121. doi:[10.1051/0004-6361/201321140](https://doi.org/10.1051/0004-6361/201321140). [arXiv:1304.4474](https://arxiv.org/abs/1304.4474)
- Falco EE (2005) A most useful manifestation of relativity: gravitational lenses. *N J Phys* 7:200. doi:[10.1088/1367-2630/7/1/200](https://doi.org/10.1088/1367-2630/7/1/200)
- Falco EE, Gorenstein MV, Shapiro II (1985) On model-dependent bounds on $H(0)$ from gravitational images application of Q0957 + 561A. *B. ApJL* 289:L1–L4. doi:[10.1086/184422](https://doi.org/10.1086/184422)
- Fassnacht CD, Pearson TJ, Readhead ACS, Browne IWA, Koopmans LVE, Myers ST, Wilkinson PN (1999) A determination of H_0 with the CLASS gravitational lens B1608+656. I. Time delay measurements with the VLA. *ApJ* 527:498–512. doi:[10.1086/308118](https://doi.org/10.1086/308118). [arXiv:astro-ph/9907257](https://arxiv.org/abs/astro-ph/9907257)
- Fassnacht CD, Xanthopoulos E, Koopmans LVE, Rusin D (2002) A determination of H_0 with the CLASS gravitational lens B1608+656. III. A significant improvement in the precision of the time delay measurements. *ApJ* 581:823–835. doi:[10.1086/344368](https://doi.org/10.1086/344368). [arXiv:astro-ph/0208420](https://arxiv.org/abs/astro-ph/0208420)
- Fassnacht CD, Gal RR, Lubin LM, McKean JP, Squires GK, Readhead ACS (2006) Mass along the line of sight to the gravitational lens B1608+656: galaxy groups and implications for H_0 . *ApJ* 642:30–38. doi:[10.1086/500927](https://doi.org/10.1086/500927). [arXiv:astro-ph/0510728](https://arxiv.org/abs/astro-ph/0510728)
- Fassnacht CD, Koopmans LVE, Wong KC (2011) Galaxy number counts and implications for strong lensing. *MNRAS* 410:2167–2179. doi:[10.1111/j.1365-2966.2010.17591.x](https://doi.org/10.1111/j.1365-2966.2010.17591.x). [arXiv:0909.4301](https://arxiv.org/abs/0909.4301)
- Fiacconi D, Madau P, Potter D, Stadel J (2016) Cold dark matter substructures in early-type galaxy halos. [arXiv:1602.03526](https://arxiv.org/abs/1602.03526)
- Fohlmeister J, Kochanek CS, Falco EE, Wambsganss J, Morgan N, Morgan CW, Ofek EO, Maoz D, Keeton CR, Barentine JC, Dalton G, Dembicky J, Ketzeback W, McMillan R, Peters CS (2007) A time delay for the cluster-lensed quasar SDSS J1004+4112. *ApJ* 662:62–71. doi:[10.1086/518018](https://doi.org/10.1086/518018)
- Freedman WL, Madore BF, Scowcroft V, Burns C, Monson A, Persson SE, Seibert M, Rigby J (2012) Carnegie Hubble program: a mid-infrared calibration of the Hubble constant. *ApJ* 758:24. doi:[10.1088/0004-637X/758/1/24](https://doi.org/10.1088/0004-637X/758/1/24). [arXiv:1208.3281](https://arxiv.org/abs/1208.3281)
- Gavazzi R (2005) Projection effects in cluster mass estimates: the case of MS2137-23. *A A* 443:793–804. doi:[10.1051/0004-6361:20053166](https://doi.org/10.1051/0004-6361:20053166)
- Greene ZS, Suyu SH, Treu T, Hilbert S, Auger MW, Collett TE, Marshall PJ, Fassnacht CD, Blandford RD, Bradač M, Koopmans LVE (2013) Improving the precision of time-delay cosmography with observations of galaxies along the line of sight. *ApJ* 768:39. doi:[10.1088/0004-637X/768/1/39](https://doi.org/10.1088/0004-637X/768/1/39). [arXiv:1303.3588](https://arxiv.org/abs/1303.3588)
- Grillo C, Lombardi M, Bertin G (2008) Cosmological parameters from strong gravitational lensing and stellar dynamics in elliptical galaxies. *A A* 477:397–406. doi:[10.1051/0004-6361:20077534](https://doi.org/10.1051/0004-6361:20077534). [arXiv:0711.0882](https://arxiv.org/abs/0711.0882)
- Grillo C, Karman W, Suyu SH, Rosati P, Balestra I, Mercurio A, Lombardi M, Treu T, Caminha GB, Halkola A, Rodney SA, Gavazzi R, Caputi KI (2016) The story of supernova Refsdal told by muse. *ApJ* 822:78. doi:[10.3847/0004-637X/822/2/78](https://doi.org/10.3847/0004-637X/822/2/78). [arXiv:1511.04093](https://arxiv.org/abs/1511.04093)
- Hainline LJ, Morgan CW, MacLeod CL, Landaal ZD, Kochanek CS, Harris HC, Tillemann T, Goicoechea LJ, Shalyapin VN, Falco EE (2013) Time delay and accretion disk size measurements in the lensed quasar SBS 0909+532 from multiwavelength microlensing analysis. *ApJ* 774:69. doi:[10.1088/0004-637X/774/1/69](https://doi.org/10.1088/0004-637X/774/1/69). [arXiv:1307.3254](https://arxiv.org/abs/1307.3254)
- Heymans C, Van Waerbeke L, Bacon D, Berge J, Bernstein G, Bertin E, Bridle S, Brown ML, Clowe D, Dahle H, Erben T, Gray M, Hettterscheidt M, Hoekstra H, Hudelot P, Jarvis M, Kuijken K, Margoniner

- V, Massey R, Mellier Y, Nakajima R, Refregier A, Rhodes J, Schrabback T, Wittman D (2006) The shear testing programme—I. Weak lensing analysis of simulated ground-based observations. *MNRAS* 368:1323–1339. doi:[10.1111/j.1365-2966.2006.10198.x](https://doi.org/10.1111/j.1365-2966.2006.10198.x). [arXiv:astro-ph/0506112](https://arxiv.org/abs/astro-ph/0506112)
- Hezaveh Y, Dalal N, Holder G, Kuhlen M, Marrone D, Murray N, Vieira J (2013a) Dark matter substructure detection using spatially resolved spectroscopy of lensed dusty galaxies. *ApJ* 767:9. doi:[10.1088/0004-637X/767/1/9](https://doi.org/10.1088/0004-637X/767/1/9). [arXiv:1210.4562](https://arxiv.org/abs/1210.4562)
- Hezaveh YD, Marrone DP, Fassnacht CD, Spilker JS, Vieira JD, Aguirre JE, Aird KA, Aravena M, Ashby MLN, Bayliss M, Benson BA, Bleem LE, Bothwell M, Brodwin M, Carlstrom JE, Chang CL, Chapman SC, Crawford TM, Crites AT, De Breuck C, de Haan T, Dobbs MA, Fomalont EB, George EM, Gladders MD, Gonzalez AH, Greve TR, Halverson NW, High FW, Holder GP, Holzappel WL, Hoover S, Hrubes JD, Husband K, Hunter TR, Keisler R, Lee AT, Leitch EM, Lueker M, Luong-Van D, Malkan M, McIntyre V, McMahon JJ, Mehl J, Menten KM, Meyer SS, Mocanu LM, Murphy EJ, Natoli T, Padin S, Plagge T, Reichardt CL, Rest A, Ruel J, Ruhl JE, Sharon K, Schaffer KK, Shaw L, Shirokoff E, Stalder B, Staniszewski Z, Stark AA, Story K, Vanderlinde K, Weißa Welikala N, Williamson R (2013b) ALMA observations of SPT-discovered, strongly lensed, dusty, star-forming galaxies. *ApJ* 767:132. doi:[10.1088/0004-637X/767/2/132](https://doi.org/10.1088/0004-637X/767/2/132). [arXiv:1303.2722](https://arxiv.org/abs/1303.2722)
- Hicken M, Wood-Vasey WM, Blondin S, Challis P, Jha S, Kelly PL, Rest A, Kirshner RP (2009) Improved dark energy constraints from ~ 100 new CfA supernova type Ia light curves. *ApJ* 700:1097–1140. doi:[10.1088/0004-637X/700/2/1097](https://doi.org/10.1088/0004-637X/700/2/1097). [arXiv:0901.4804](https://arxiv.org/abs/0901.4804)
- Hilbert S, Hartlap J, White SDM, Schneider P (2009) Ray-tracing through the millennium simulation: born corrections and lens-lens coupling in cosmic shear and galaxy-galaxy lensing. *A A* 499:31–43. doi:[10.1051/0004-6361/200811054](https://doi.org/10.1051/0004-6361/200811054). [arXiv:0809.5035](https://arxiv.org/abs/0809.5035)
- Hjorth J, Burud I, Jaunsen AO, Schechter PL, Kneib JP, Andersen MI, Korhonen H, Clasen JW, Kaas AA, Østensen R, Pelt J, Pijpers FP (2002) The time delay of the quadruple quasar RX J0911.4+0551. *APJL* 572:L11–L14. doi:[10.1086/341603](https://doi.org/10.1086/341603). [arXiv:astro-ph/0205124](https://arxiv.org/abs/astro-ph/0205124)
- Hojjati A, Linder EV (2014) Next generation strong lensing time delay estimation with Gaussian processes. *Phys. Rev. D* 90(12):123501. doi:[10.1103/PhysRevD.90.123501](https://doi.org/10.1103/PhysRevD.90.123501). [arXiv:1408.5143](https://arxiv.org/abs/1408.5143)
- Holz DE (2001) Seeing double: strong gravitational lensing of high-redshift supernovae. *ApJL* 556:L71–L74. doi:[10.1086/322947](https://doi.org/10.1086/322947). [arXiv:astro-ph/0104440](https://arxiv.org/abs/astro-ph/0104440)
- Hu W (2005) Dark energy probes in light of the CMB. In: Wolff SC, Lauer TR (eds) Observing dark energy, Astronomical Society of the Pacific Conference Series, vol 339, p 215. [arXiv:astro-ph/0407158](https://arxiv.org/abs/astro-ph/0407158)
- Jackson N (2013) Quasar lensing. [arXiv:1304.4172](https://arxiv.org/abs/1304.4172)
- Jackson N (2015) The Hubble constant. *Living Rev Relativ*, p 18. doi:[10.1007/lrr-2015-2](https://doi.org/10.1007/lrr-2015-2)
- Jakobsson P, Hjorth J, Burud I, Letawe G, Lidman C, Courbin F (2005) An optical time delay for the double gravitational lens system FBQ 0951+2635. *A A* 431:103–109. doi:[10.1051/0004-6361:20041432](https://doi.org/10.1051/0004-6361:20041432). [arXiv:astro-ph/0409444](https://arxiv.org/abs/astro-ph/0409444)
- Jauzac M, Richard J, Limousin M, Knowles K, Mahler G, Smith GP, Kneib JP, Jullo E, Natarajan P, Ebeling H, Atek H, Clément B, Eckert D, Egami E, Massey R, Rexroth M (2016) Hubble frontier fields: predictions for the return of SN Refsdal with the MUSE and GMOS spectrographs. *MNRAS* 457:2029–2042. doi:[10.1093/mnras/stw069](https://doi.org/10.1093/mnras/stw069). [arXiv:1509.08914](https://arxiv.org/abs/1509.08914)
- Jee I, Komatsu E, Suyu SH (2015) Measuring angular diameter distances of strong gravitational lenses. *JCAP* 11:033. doi:[10.1088/1475-7516/2015/11/033](https://doi.org/10.1088/1475-7516/2015/11/033). [arXiv:1410.7770](https://arxiv.org/abs/1410.7770)
- Jee I, Komatsu E, Suyu SH, Huterer D (2016) Time-delay cosmography: increased leverage with angular diameter distances. *JCAP* 4:031. doi:[10.1088/1475-7516/2016/04/031](https://doi.org/10.1088/1475-7516/2016/04/031). [arXiv:1509.03310](https://arxiv.org/abs/1509.03310)
- Kawamata R, Oguri M, Ishigaki M, Shimasaku K, Ouchi M (2016) Precise strong lensing mass modeling of four Hubble frontier field clusters and a sample of magnified high-redshift galaxies. *ApJ* 819:114. doi:[10.3847/0004-637X/819/2/114](https://doi.org/10.3847/0004-637X/819/2/114). [arXiv:1510.06400](https://arxiv.org/abs/1510.06400)
- Keeton CR (2011) GRAVLENS: computational methods for gravitational lensing. *Astrophysics Source Code Library*. [arXiv:1102.003](https://arxiv.org/abs/1102.003)
- Keeton CR, Moustakas LA (2009) A new channel for detecting dark matter substructure in galaxies: gravitational lens time delays. *ApJ* 699:1720–1731. doi:[10.1088/0004-637X/699/2/1720](https://doi.org/10.1088/0004-637X/699/2/1720). [arXiv:0805.0309](https://arxiv.org/abs/0805.0309)
- Keeton CR, Zabludoff AI (2004) The importance of lens galaxy environments. *ApJ* 612:660–678. doi:[10.1086/422745](https://doi.org/10.1086/422745). [arXiv:astro-ph/0406060](https://arxiv.org/abs/astro-ph/0406060)
- Keeton CR, Falco EE, Impey CD, Kochanek CS, Lehár J, McLeod BA, Rix HW, Muñoz JA, Peng CY (2000) The host galaxy of the lensed quasar q0957+561. *Astrophys J* 542:74. doi:[10.1086/309517](https://doi.org/10.1086/309517)
- Kelly PL, Rodney SA, Treu T, Foley RJ, Brammer G, Schmidt KB, Zitrin A, Sonnenfeld A, Strolger LG, Graur O, Filippenko AV, Jha SW, Riess AG, Bradac M, Weiner BJ, Scolnic D, Malkan MA, von der

- Linden A, Trenti M, Hjorth J, Gavazzi R, Fontana A, Merten JC, McCully C, Jones T, Postman M, Dressler A, Patel B, Cenko SB, Graham ML, Tucker BE (2015) Multiple images of a highly magnified supernova formed by an early-type cluster galaxy lens. *Science* 347:1123–1126. doi:[10.1126/science.aaa3350](https://doi.org/10.1126/science.aaa3350). [arXiv:1411.6009](https://arxiv.org/abs/1411.6009)
- Kelly PL, Rodney SA, Treu T, Strolger LG, Foley RJ, Jha SW, Selsing J, Brammer G, Bradač M, Cenko SB, Graur O, Filippenko AV, Hjorth J, McCully C, Molino A, Nonino M, Riess AG, Schmidt KB, Tucker B, von der Linden A, Weiner BJ, Zitrin A (2016) Deja Vu all over again: the reappearance of supernova Refsdal. *ApJL* 819:L8. doi:[10.3847/2041-8205/819/1/L8](https://doi.org/10.3847/2041-8205/819/1/L8). [arXiv:1512.04654](https://arxiv.org/abs/1512.04654)
- Kim AG, Padmanabhan N, Aldering G, Allen SW, Baltay C, Cahn RN, D'Andrea CB, Dalal N, Dawson KS, Denney KD, Eisenstein DJ, Finley DA, Freedman WL, Ho S, Holz DE, Kasen D, Kent SM, Kessler R, Kuhlmann S, Linder EV, Martini P, Nugent PE, Perlmutter S, Peterson BM, Riess AG, Rubin D, Sako M, Suntzeff NV, Suzuki N, Thomas RC, Wood-Vasey WM, Woosley SE (2015) Distance probes of dark energy. *Astrophys J* 63:2–22. doi:[10.1016/j.astrophys.2014.05.007](https://doi.org/10.1016/j.astrophys.2014.05.007). [arXiv:1309.5382](https://arxiv.org/abs/1309.5382)
- Klein JR, Roodman A (2005) Blind analysis in nuclear and particle physics. *Annu Rev Nucl Part Sci* 55:141–163
- Kneib JP, Bonnet H, Golse G, Sand D, Jullo E, Marshall P (2011) LENSTOOL: a gravitational lensing software for modeling mass distribution of galaxies and clusters (strong and weak regime). *Astrophysics Source Code Library*. [arXiv:1102.004](https://arxiv.org/abs/1102.004)
- Kochanek CS (2002) What do gravitational lens time delays measure? *ApJ* 578:25–32. doi:[10.1086/342476](https://doi.org/10.1086/342476). [arXiv:astro-ph/0205319](https://arxiv.org/abs/astro-ph/0205319)
- Kochanek CS, Schechter PL (2004) The Hubble constant from gravitational lens time delays. *Measuring and modeling the universe*, p 117. [arXiv:astro-ph/0306040](https://arxiv.org/abs/astro-ph/0306040)
- Kochanek CS, Keeton CR, McLeod BA (2001) The importance of Einstein rings. *APJ* 547:50–59. doi:[10.1086/318350](https://doi.org/10.1086/318350). [arXiv:astro-ph/0006116](https://arxiv.org/abs/astro-ph/0006116)
- Kolatt TS, Bartelmann M (1998) Gravitational lensing of type IA supernovae by galaxy clusters. *MNRAS* 296:763–772. doi:[10.1046/j.1365-8711.1998.01466.x](https://doi.org/10.1046/j.1365-8711.1998.01466.x). [arXiv:astro-ph/9708120](https://arxiv.org/abs/astro-ph/9708120)
- Koopmans LVE (2005) Gravitational imaging of cold dark matter substructures. *MNRAS* 363:1136–1144. doi:[10.1111/j.1365-2966.2005.09523.x](https://doi.org/10.1111/j.1365-2966.2005.09523.x)
- Koopmans LVE, Fassnacht CD (1999) A Determination of H_0 with the CLASS gravitational lens B1608+656. II. Mass models and the Hubble constant from lensing. *ApJ* 527:513–524. doi:[10.1086/308120](https://doi.org/10.1086/308120). [arXiv:astro-ph/9907258](https://arxiv.org/abs/astro-ph/9907258)
- Koopmans LVE, Treu T, Fassnacht CD, Blandford RD, Surpi G (2003) The Hubble constant from the gravitational lens B1608+656. *ApJ* 599:70–85. doi:[10.1086/379226](https://doi.org/10.1086/379226). [arXiv:astro-ph/0306216](https://arxiv.org/abs/astro-ph/0306216)
- Koopmans LVE, Bolton A, Treu T, Czoske O, Auger MW, Barnabè M, Vegetti S, Gavazzi R, Moustakas LA, Bures S (2009) The structure and dynamics of massive early-type galaxies: on homology, isothermality, and isotropy inside one effective radius. *ApJL* 703:L51–L54. doi:[10.1088/0004-637X/703/1/L51](https://doi.org/10.1088/0004-637X/703/1/L51). [arXiv:0906.1349](https://arxiv.org/abs/0906.1349)
- Kundic T, Turner EL, Colley WN, Gott JRI, Rhoads JE, Wang Y, Bergeron LE, Gloria KA, Long DC, Malhotra S, Wambsgans J (1997) A robust determination of the time delay in 0957+561A, B and a measurement of the global value of Hubble's constant. *APJ* 482:75. doi:[10.1086/304147](https://doi.org/10.1086/304147). [arXiv:astro-ph/9610162](https://arxiv.org/abs/astro-ph/9610162)
- Lewis GF, Ibata RA (2002) An investigation of gravitational lens determinations of H_0 in quintessence cosmologies. *MNRAS* 337:26–33. doi:[10.1046/j.1365-8711.2002.05797.x](https://doi.org/10.1046/j.1365-8711.2002.05797.x). [arXiv:astro-ph/0206425](https://arxiv.org/abs/astro-ph/0206425)
- Liao K, Treu T, Marshall P, Fassnacht CD, Rumbaugh N, Dobler G, Aghamousa A, Bonvin V, Courbin F, Hojjati A, Jackson N, Kashyap V, Rathna Kumar S, Linder E, Mandel K, Meng XL, Meylan G, Moustakas LA, Prabhu TP, Romero-Wolf A, Shafieloo A, Siemiginowska A, Stalin CS, Tak H, Tewes M, van Dyk D (2015) Strong lens time delay challenge. II. Results of TDC1. *ApJ* 800:11. doi:[10.1088/0004-637X/800/1/11](https://doi.org/10.1088/0004-637X/800/1/11). [arXiv:1409.1254](https://arxiv.org/abs/1409.1254)
- Linder EV (2011) Lensing time delays and cosmological complementarity. *Phys. Rev. D* 84(12):123529. doi:[10.1103/PhysRevD.84.123529](https://doi.org/10.1103/PhysRevD.84.123529). [arXiv:1109.2592](https://arxiv.org/abs/1109.2592)
- Linder EV (2015) Tailoring strong lensing cosmographic observations. *Phys. Rev. D* 91(8):083511. doi:[10.1103/PhysRevD.91.083511](https://doi.org/10.1103/PhysRevD.91.083511). [arXiv:1502.01353](https://arxiv.org/abs/1502.01353)
- MacLeod CL, Morgan CW, Mosquera A, Kochanek CS, Tewes M, Courbin F, Meylan G, Chen B, Dai X, Chartas G (2015) A consistent picture emerges: a compact X-ray continuum emission region in the gravitationally lensed quasar SDSS J0924+0219. *ApJ* 806:258. doi:[10.1088/0004-637X/806/2/258](https://doi.org/10.1088/0004-637X/806/2/258). [arXiv:1501.07533](https://arxiv.org/abs/1501.07533)

- Magain P, Courbin F, Sohy S (1998) Deconvolution with correct sampling. *ApJ* 494:472–477. doi:[10.1086/305187](https://doi.org/10.1086/305187). [arXiv:astro-ph/9704059](https://arxiv.org/abs/astro-ph/9704059)
- Marshall PJ et al (2007) Superresolving distant galaxies with gravitational telescopes: keck laser guide star adaptive optics and hubble space telescope imaging of the lens system SDSS J0737+3216. *ApJ* 671:1196–1211. doi:[10.1086/523091](https://doi.org/10.1086/523091). [arXiv:0710.0637](https://arxiv.org/abs/0710.0637)
- McCully C, Keeton CR, Wong KC, Zabludoff AI (2014) A new hybrid framework to efficiently model lines of sight to gravitational lenses. *MNRAS* 443:3631–3642. doi:[10.1093/mnras/stu1316](https://doi.org/10.1093/mnras/stu1316). [arXiv:1401.0197](https://arxiv.org/abs/1401.0197)
- McCully C, Keeton CR, Wong KC, Zabludoff AI (2016) Quantifying environmental and line-of-sight effects in models of strong gravitational lens systems. [arXiv:1601.05417](https://arxiv.org/abs/1601.05417)
- Meng XL, Treu T, Agnello A, Auger MW, Liao K, Marshall PJ (2015) Precision cosmology with time delay lenses: high resolution imaging requirements. *JCAP* 9:059. doi:[10.1088/1475-7516/2015/09/059](https://doi.org/10.1088/1475-7516/2015/09/059), [arXiv:1506.07640](https://arxiv.org/abs/1506.07640)
- Metcalf RB (2005) Testing Λ CDM with gravitational lensing constraints on small-scale structure. *Astrophys J* 622(72):2005. doi:[10.1086/427864](https://doi.org/10.1086/427864), (c) 2005: The American Astronomical Society
- Metcalf RB, Madau P (2001) Compound gravitational lensing as a probe of dark matter substructure within galaxy halos. *ApJ* 563:9–20. doi:[10.1086/323695](https://doi.org/10.1086/323695). [arXiv:astro-ph/0108224](https://arxiv.org/abs/astro-ph/0108224)
- Momcheva I, Williams K, Keeton C, Zabludoff A (2006) A spectroscopic study of the environments of gravitational lens galaxies. *ApJ* 641:169–189. doi:[10.1086/500382](https://doi.org/10.1086/500382). [arXiv:astro-ph/0511594](https://arxiv.org/abs/astro-ph/0511594)
- Momcheva IG, Williams KA, Cool RJ, Keeton CR, Zabludoff AI (2015) A spectroscopic survey of the fields of 28 strong gravitational lenses. *ApJs* 219:29. doi:[10.1088/0067-0049/219/2/29](https://doi.org/10.1088/0067-0049/219/2/29), [arXiv:1503.02074](https://arxiv.org/abs/1503.02074)
- More A, Oguri M, Kayo I, Zinn J, Strauss MA, Santiago BX, Mosquera AM, Inada N, Kochanek CS, Rusu CE, Brownstein JR, da Costa LN, Kneib JP, Maia MAG, Quimby RM, Schneider DP, Streblyanska A, York DG (2016) The SDSS-III BOSS quasar lens survey: discovery of 13 gravitationally lensed quasars. *MNRAS* 456:1595–1606. doi:[10.1093/mnras/stv2813](https://doi.org/10.1093/mnras/stv2813), [arXiv:1509.07917](https://arxiv.org/abs/1509.07917)
- Moustakas LA, Bolton AJ, Booth JT, Bullock JS, Cheng E, Coe D, Fassnacht CD, Gorjian V, Heneghan C, Keeton CR, Kochanek CS, Lawrence CR, Marshall PJ, Metcalf RB, Natarajan P, Nikzad S, Peterson BM, Wambsganss J (2008) The observatory for multi-epoch gravitational lens astrophysics (OMEGA). In: *Space telescopes and instrumentation 2008: optical, infrared, and millimeter*, *PROC SPIE*, vol 7010, p 70101B. doi:[10.1117/12.789987](https://doi.org/10.1117/12.789987), [arXiv:0806.1884](https://arxiv.org/abs/0806.1884)
- Newton ER, Marshall PJ, Treu T, Auger MW, Gavazzi R, Bolton AS, Koopmans LVE, Moustakas LA (2011) The sloan lens ACS survey. XI. Beyond Hubble resolution: size, luminosity, and stellar mass of compact lensed galaxies at intermediate redshift. *ApJ* 734:104. doi:[10.1088/0004-637X/734/2/104](https://doi.org/10.1088/0004-637X/734/2/104), [arXiv:1104.2608](https://arxiv.org/abs/1104.2608)
- Nierenberg AM, Treu T, Wright SA, Fassnacht CD, Auger MW (2014) Detection of substructure with adaptive optics integral field spectroscopy of the gravitational lens B1422+231. *MNRAS* 442:2434–2445. doi:[10.1093/mnras/stu862](https://doi.org/10.1093/mnras/stu862). [arXiv:1402.1496](https://arxiv.org/abs/1402.1496)
- Nightingale JW, Dye S (2015) Adaptive semi-linear inversion of strong gravitational lens imaging. *MNRAS* 452:2940–2959. doi:[10.1093/mnras/stv1455](https://doi.org/10.1093/mnras/stv1455). [arXiv:1412.7436](https://arxiv.org/abs/1412.7436)
- Nordin J, Rubin D, Richard J, Rykoff E, Aldering G, Amanullah R, Atek H, Barbary K, Deustua S, Fakhouri HK, Fruchter AS, Goobar A, Hook I, Hsiao EY, Huang X, Kneib JP, Lidman C, Meyers J, Perlmutter S, Saunders C, Spadafora AL, Suzuki N (2014) Supernova cosmology project lensed type Ia supernovae as probes of cluster mass models. *MNRAS* 440:2742–2754. doi:[10.1093/mnras/stu376](https://doi.org/10.1093/mnras/stu376). [arXiv:1312.2576](https://arxiv.org/abs/1312.2576)
- Oguri M (2007) Gravitational lens time delays: a statistical assessment of lens model dependences and implications for the global Hubble constant. *ApJ* 660:1–15. doi:[10.1086/513093](https://doi.org/10.1086/513093). [arXiv:astro-ph/0609694](https://arxiv.org/abs/astro-ph/0609694)
- Oguri M (2015) Predicted properties of multiple images of the strongly lensed supernova SN Refsdal. *MNRAS* 449:L86–L89. doi:[10.1093/mnras/slv025](https://doi.org/10.1093/mnras/slv025). [arXiv:1411.6443](https://arxiv.org/abs/1411.6443)
- Oguri M, Marshall PJ (2010) Gravitationally lensed quasars and supernovae in future wide-field optical imaging surveys. *MNRAS* 405:2579–2593. doi:[10.1111/j.1365-2966.2010.16639.x](https://doi.org/10.1111/j.1365-2966.2010.16639.x), [arXiv:1001.2037](https://arxiv.org/abs/1001.2037)
- Oguri M, Inada N, Pindor B, Strauss MA, Richards GT, Hennawi JF, Turner EL, Lupton RH, Schneider DP, Fukugita M, Brinkmann J (2006) The sloan digital sky survey quasar lens search. i. candidate selection algorithm. *Astron J* 132:999. doi:[10.1086/506019](https://doi.org/10.1086/506019)
- Paraficz D, Hjorth J (2009) Gravitational lenses as cosmic rulers: Ω_m , Ω from time delays and velocity dispersions. *A A* 507:L49–L52. doi:[10.1051/0004-6361/200913307](https://doi.org/10.1051/0004-6361/200913307). [arXiv:0910.5823](https://arxiv.org/abs/0910.5823)
- Paraficz D, Hjorth J (2010) The Hubble constant inferred from 18 time-delay lenses. *ApJ* 712:1378–1384. doi:[10.1088/0004-637X/712/2/1378](https://doi.org/10.1088/0004-637X/712/2/1378). [arXiv:1002.2570](https://arxiv.org/abs/1002.2570)

- Patel B, McCully C, Jha SW, Rodney SA, Jones DO, Graur O, Merten J, Zitrin A, Riess AG, Matheson T, Sako M, Holoiien TWS, Postman M, Coe D, Bartelmann M, Balestra I, Benítez N, Bouwens R, Bradley L, Broadhurst T, Cenko SB, Donahue M, Filippenko AV, Ford H, Garnavich P, Grillo C, Infante L, Jouvel S, Kelson D, Koekemoer A, Lahav O, Lemze D, Maoz D, Medezinski E, Melchior P, Meneghetti M, Molino A, Moustakas J, Moustakas LA, Nonino M, Rosati P, Seitz S, Strolger LG, Umetsu K, Zheng W (2014) Three gravitationally lensed supernovae behind CLASH galaxy clusters. *ApJ* 786:9. doi:[10.1088/0004-637X/786/1/9](https://doi.org/10.1088/0004-637X/786/1/9). [arXiv:1312.0943](https://arxiv.org/abs/1312.0943)
- Pelt J, Kayser R, Refsdal S, Schramm T (1996) The light curve and the time delay of QSO 0957+561. *A A* 305:97 [arXiv:astro-ph/9501036](https://arxiv.org/abs/astro-ph/9501036)
- Percival WJ, Reid BA, Eisenstein DJ, Bahcall NA, Budavari T, Frieman JA, Fukugita M, Gunn JE, Ivezić Ž, Knapp GR, Kron RG, Loveday J, Lupton RH, McKay TA, Meiksin A, Nichol RC, Pope AC, Schlegel DJ, Schneider DP, Spergel DN, Stoughton C, Strauss MA, Szalay AS, Tegmark M, Vogeley MS, Weinberg DH, York DG, Zehavi I (2010) Baryon acoustic oscillations in the sloan digital sky survey data release 7 galaxy sample. *MNRAS* 401:2148–2168. doi:[10.1111/j.1365-2966.2009.15812.x](https://doi.org/10.1111/j.1365-2966.2009.15812.x). [arXiv:0907.1660](https://arxiv.org/abs/0907.1660)
- Perlick V (1990a) On Fermat's principle in general relativity. I. The general case. *Class Quant Grav* 7:1319–1331. doi:[10.1088/0264-9381/7/8/011](https://doi.org/10.1088/0264-9381/7/8/011)
- Perlick V (1990b) On Fermat's principle in general relativity. II. The conformally stationary case. *Class Quant Grav* 7:1849–1867. doi:[10.1088/0264-9381/7/10/016](https://doi.org/10.1088/0264-9381/7/10/016)
- Perlmutter S, Aldering G, Goldhaber G, Knop RA, Nugent P, Castro PG, Deustua S, Fabbro S, Goobar A, Groom DE, Hook IM, Kim AG, Kim MY, Lee JC, Nunes NJ, Pain R, Pennypacker CR, Quimby R, Lidman C, Ellis RS, Irwin M, McMahon RG, Ruiz-Lapuente P, Walton N, Schaefer B, Boyle BJ, Filippenko AV, Matheson T, Fruchter AS, Panagia N, Newberg HJM, Couch WJ (1999) The supernova cosmology project measurements of omega and lambda from 42 high-redshift supernovae. *ApJ* 517:565–586. doi:[10.1086/307221](https://doi.org/10.1086/307221). [arXiv:astro-ph/9812133](https://arxiv.org/abs/astro-ph/9812133)
- Petters AO, Levine H, Wambsganss J (2001) Singularity theory and gravitational lensing, *Progress in mathematical physics* v.21. Birkhäuser, Boston
- Planck Collaboration, Ade PAR, Aghanim N, Arnaud M, Ashdown M, Aumont J, Baccigalupi C, Banday AJ, Barreiro RB, Bartlett JG, et al (2015) Planck 2015 results. XIII. Cosmological parameters. [arXiv:1502.01589](https://arxiv.org/abs/1502.01589)
- Poindexter S, Morgan N, Kochanek CS, Falco EE (2007) Mid-IR observations and a revised time delay for the gravitational lens system quasar HE 1104–1805. *ApJ* 660:146–151. doi:[10.1086/512773](https://doi.org/10.1086/512773). [arXiv:astro-ph/0612045](https://arxiv.org/abs/astro-ph/0612045)
- Poindexter S, Morgan N, Kochanek CS (2008) The spatial structure of an accretion disk. *ApJ* 673:34–38. doi:[10.1086/524190](https://doi.org/10.1086/524190). [arXiv:0707.0003](https://arxiv.org/abs/0707.0003)
- Press WH, Rybicki GB, Hewitt JN (1992) The time delay of gravitational lens 0957+561. II. Analysis of radio data and combined optical-radio analysis. *ApJ* 385:416. doi:[10.1086/170952](https://doi.org/10.1086/170952)
- Quimby RM, Oguri M, More A, More S, Moriya TJ, Werner MC, Tanaka M, Folatelli G, Bersten MC, Maeda K, Nomoto K (2014) Detection of the gravitational lens magnifying a type Ia supernova. *Science* 344:396–399. doi:[10.1126/science.1250903](https://doi.org/10.1126/science.1250903). [arXiv:1404.6014](https://arxiv.org/abs/1404.6014)
- Rathna Kumar S, Tewes M, Stalin CS, Courbin F, Asfandiyarov I, Meylan G, Eulaers E, Prabhu TP, Magain P, Van Winckel H, Ehgamberdiev S (2013) COSMOGRAIL: the COSmological MONitoring of GRAvitational Lenses. XIV. Time delay of the doubly lensed quasar SDSS J1001+5027. *A A* 557:A44. doi:[10.1051/0004-6361/201322116](https://doi.org/10.1051/0004-6361/201322116). [arXiv:1306.5105](https://arxiv.org/abs/1306.5105)
- Rathna Kumar S, Stalin CS, Prabhu TP (2015) H_0 from ten well-measured time delay lenses. *A A* 580:A38. doi:[10.1051/0004-6361/201423977](https://doi.org/10.1051/0004-6361/201423977). [arXiv:1404.2920](https://arxiv.org/abs/1404.2920)
- Read JI, Saha P, Macciò AV (2007) Radial density profiles of time-delay lensing galaxies. *ApJ* 667:645–654. doi:[10.1086/520714](https://doi.org/10.1086/520714). [arXiv:0704.3267](https://arxiv.org/abs/0704.3267)
- Refsdal S (1964) On the possibility of determining Hubble's parameter and the masses of galaxies from the gravitational lens effect. *MNRAS* 128:307
- Riess AG, Filippenko AV, Challis P, Clocchiatti A, Diercks A, Garnavich PM, Gilliland RL, Hogan CJ, Jha S, Kirshner RP, Leibundgut B, Phillips MM, Reiss D, Schmidt BP, Schommer RA, Smith RC, Spyromilio J, Stubbs C, Suntzeff NB, Tonry J (1998) Observational evidence from supernovae for an accelerating universe and a cosmological constant. *Astron J* 116:1009. doi:[10.1086/300499](https://doi.org/10.1086/300499)
- Riess AG, Macri LM, Hoffmann SL, Scolnic D, Casertano S, Filippenko AV, Tucker BE, Reid MJ, Jones DO, Silverman JM, Chornock R, Challis P, Yuan W, Foley RJ (2016) A 2.4% determination of the local value of the Hubble constant. [arXiv:1604.01424](https://arxiv.org/abs/1604.01424)

- Rigault M, Aldering G, Kowalski M, Copin Y, Antilogus P, Aragon C, Bailey S, Baltay C, Baugh D, Bongard S, Boone K, Buton C, Chen J, Chotard N, Fakhouri HK, Feindt U, Fagrelis P, Fleury M, Fouchez D, Gangler E, Hayden B, Kim AG, Leget PF, Lombardo S, Nordin J, Pain R, Pecontal E, Pereira R, Perlmutter S, Rabinowitz D, Runge K, Rubin D, Saunders C, Smadja G, Sofiatti C, Suzuki N, Tao C, Weaver BA (2015) Confirmation of a star formation bias in type Ia supernova distances and its effect on the measurement of the Hubble constant. *ApJ* 802:20. doi:[10.1088/0004-637X/802/1/20](https://doi.org/10.1088/0004-637X/802/1/20). [arXiv:1412.6501](https://arxiv.org/abs/1412.6501)
- Rodney SA, Patel B, Scolnic D, Foley RJ, Molino A, Brammer G, Jauzac M, Bradač M, Broadhurst T, Coe D, Diego JM, Graur O, Hjorth J, Hoag A, Jha SW, Johnson TL, Kelly P, Lam D, McCully C, Medezinski E, Meneghetti M, Merten J, Richard J, Riess A, Sharon K, Strolger LG, Treu T, Wang X, Williams LLR, Zitrin A (2015) Illuminating a dark lens : a type Ia supernova magnified by the frontier fields galaxy cluster abell 2744. *ApJ* 811:70. doi:[10.1088/0004-637X/811/1/70](https://doi.org/10.1088/0004-637X/811/1/70). [arXiv:1505.06211](https://arxiv.org/abs/1505.06211)
- Rodney SA, Strolger LG, Kelly PL, Bradač M, Brammer G, Filippenko AV, Foley RJ, Graur O, Hjorth J, Jha SW, McCully C, Molino A, Riess AG, Schmidt KB, Selsing J, Sharon K, Treu T, Weiner BJ, Zitrin A (2016) SN Refsdal: photometry and time delay measurements of the first Einstein cross supernova. *APJ* 820:50. doi:[10.3847/0004-637X/820/1/50](https://doi.org/10.3847/0004-637X/820/1/50). [arXiv:1512.05734](https://arxiv.org/abs/1512.05734)
- Rusu CE, Oguri M, Minowa Y, Iye M, Inada N, Oya S, Kayo I, Hayano Y, Hattori M, Saito Y, Ito M, Pyo TS, Terada H, Takami H, Watanabe M (2016) Subaru Telescope adaptive optics observations of gravitationally lensed quasars in the sloan digital sky survey. *MNRAS* 458:2–55. doi:[10.1093/mnras/stw092](https://doi.org/10.1093/mnras/stw092), [arXiv:1506.05147](https://arxiv.org/abs/1506.05147)
- Saha P, Coles J, Macciò AV, Williams LLR (2006) The Hubble time inferred from 10 time delay lenses. *ApJL* 650:L17–L20. doi:[10.1086/507583](https://doi.org/10.1086/507583). [arXiv:astro-ph/0607240](https://arxiv.org/abs/astro-ph/0607240)
- Schechter PL, Bailyn CD, Barr R, Barvainis R, Becker CM, Bernstein GM, Blakeslee JP, Bus SJ, Dressler A, Falco EE, Fesen RA, Fischer P, Gebhardt K, Harmer D, Hewitt JN, Hjorth J, Hurt T, Jaunsen AO, Mateo M, Mehlert D, Richstone DO, Sparke LS, Thorstensen JR, Tonry JL, Wegner G, Willmarth DW, Worthey G (1997) The quadruple gravitational lens PG 1115+080: time delays and models. *APJL* 475:L85–L88. doi:[10.1086/310478](https://doi.org/10.1086/310478). [arXiv:astro-ph/9611051](https://arxiv.org/abs/astro-ph/9611051)
- Schechter PL, Pooley D, Blackburne JA, Wambsganss J (2014) A calibration of the stellar mass fundamental plane at $z \sim 0.5$ using the micro-lensing-induced flux ratio anomalies of macro-lensed quasars. *ApJ* 793:96. doi:[10.1088/0004-637X/793/2/96](https://doi.org/10.1088/0004-637X/793/2/96). [arXiv:1405.0038](https://arxiv.org/abs/1405.0038)
- Schmidt KB, Rix HW, Shields JC, Knecht M, Hogg DW, Maoz D, Bovy J (2012) The color variability of quasars. *ApJ* 744:147. doi:[10.1088/0004-637X/744/2/147](https://doi.org/10.1088/0004-637X/744/2/147). [arXiv:1109.6653](https://arxiv.org/abs/1109.6653)
- Schneider P (1985) A new formulation of gravitational lens theory, time-delay, and Fermat's principle. *A* 143:413–420
- Schneider P (2014) Generalized multi-plane gravitational lensing: time delays, recursive lens equation, and the mass-sheet transformation. [arXiv:1409.0015](https://arxiv.org/abs/1409.0015)
- Schneider P, Sluse D (2013) Mass-sheet degeneracy, power-law models and external convergence: Impact on the determination of the Hubble constant from gravitational lensing. *A* 559:A37. doi:[10.1051/0004-6361/201321882](https://doi.org/10.1051/0004-6361/201321882). [arXiv:1306.0901](https://arxiv.org/abs/1306.0901)
- Schneider P, Sluse D (2014) Source-position transformation: an approximate invariance in strong gravitational lensing. *A* 564:A103. doi:[10.1051/0004-6361/201322106](https://doi.org/10.1051/0004-6361/201322106). [arXiv:1306.4675](https://arxiv.org/abs/1306.4675)
- Schneider P, Ehlers J, Falco EE (1992) Gravitational lenses. Springer-Verlag, Berlin, Heidelberg, New York
- Schneider P, Kochanek CS, Wambsganss J (2006) Gravitational lensing: strong, weak and micro. doi:[10.1007/978-3-540-30310-7](https://doi.org/10.1007/978-3-540-30310-7)
- Sharon K, Johnson TL (2015) Revised lens model for the multiply imaged lensed supernova Refsdal in MACS J1149+2223. *ApJL* 800:L26. doi:[10.1088/2041-8205/800/2/L26](https://doi.org/10.1088/2041-8205/800/2/L26). [arXiv:1411.6933](https://arxiv.org/abs/1411.6933)
- Skidmore W, TMT International Science Development Teams, Science Advisory Committee (2015) Thirty meter telescope detailed science case: 2015. *Res Astron Astrophys* 15:1945. doi:[10.1088/1674-4527/15/12/001](https://doi.org/10.1088/1674-4527/15/12/001). [arXiv:1505.01195](https://arxiv.org/abs/1505.01195)
- Sonnenfeld A, Bertin G, Lombardi M (2011) Direct measurement of the magnification produced by galaxy clusters as gravitational lenses. *A* 532:A37. doi:[10.1051/0004-6361/201016309](https://doi.org/10.1051/0004-6361/201016309). [arXiv:1106.1442](https://arxiv.org/abs/1106.1442)
- Sonnenfeld A, Treu T, Gavazzi R, Marshall PJ, Auger MW, Suyu SH, Koopmans LVE, Bolton AS (2012) Evidence for dark matter contraction and a salpeter initial mass function in a massive early-type galaxy. *ApJ* 752:163. doi:[10.1088/0004-637X/752/2/163](https://doi.org/10.1088/0004-637X/752/2/163). [arXiv:1111.4215](https://arxiv.org/abs/1111.4215)
- Sonnenfeld A, Treu T, Marshall PJ, Suyu SH, Gavazzi R, Auger MW, Nipoti C (2015) The SL2S galaxy-scale lens sample. V Dark matter Halos and Stellar IMF of massive early-type galaxies out to redshift 0.8. *ApJ* 800:94. doi:[10.1088/0004-637X/800/2/94](https://doi.org/10.1088/0004-637X/800/2/94). [arXiv:1410.1881](https://arxiv.org/abs/1410.1881)

- Spergel DN, Flauger R, Hlozek R (2015) Planck data reconsidered. *Phys. Rev. D* 91(2):023518. doi:[10.1103/PhysRevD.91.023518](#). [arXiv:1312.3313](#)
- Sun YH, Wang JX, Chen XY, Zheng ZY (2014) The discovery of timescale-dependent color variability of quasars. *ApJ* 792:54. doi:[10.1088/0004-637X/792/1/54](#). [arXiv:1407.4230](#)
- Suyu SH (2012) Cosmography from two-image lens systems: overcoming the lens profile slope degeneracy. *MNRAS* 426:868–879. doi:[10.1111/j.1365-2966.2012.21661.x](#). [arXiv:1202.0287](#)
- Suyu SH, Halkola A (2010) The halos of satellite galaxies: the companion of the massive elliptical lens SL2S J08544–0121. *A A* 524:A94. doi:[10.1051/0004-6361/201015481](#). [arXiv:1007.4815](#)
- Suyu SH, Marshall PJ, Hobson MP, Blandford RD (2006) A Bayesian analysis of regularized source inversions in gravitational lensing. *MNRAS* 371:983–998. doi:[10.1111/j.1365-2966.2006.10733.x](#). [arXiv:astro-ph/0601493](#)
- Suyu SH, Marshall PJ, Blandford RD, Fassnacht CD, Koopmans LVE, McKean JP, Treu T (2009) Dissecting the gravitational lens B1608+656. I. Lens potential reconstruction. *ApJ* 691:277–298. doi:[10.1088/0004-637X/691/1/277](#). [arXiv:0804.2827](#)
- Suyu SH, Marshall PJ, Auger MW, Hilbert S, Blandford RD, Koopmans LVE, Fassnacht CD, Treu T (2010) Dissecting the gravitational lens B1608+656. II. Precision measurements of the Hubble constant, spatial curvature, and the dark energy equation of state. *ApJ* 711:201–221. doi:[10.1088/0004-637X/711/1/201](#). [arXiv:0910.2773](#)
- Suyu SH, Treu T, Blandford RD, Freedman WL, Hilbert S, Blake C, Braatz J, Courbin F, Dunkley J, Greenhill L, Humphreys E, Jha S, Kirshner R, Lo KY, Macri L, Madore BF, Marshall PJ, Meylan G, Mould J, Reid B, Reid M, Riess A, Schlegel D, Scowcroft V, Verde L (2012) The Hubble constant and new discoveries in cosmology. [arXiv:1202.4459](#)
- Suyu SH, Auger MW, Hilbert S, Marshall PJ, Tewes M, Treu T, Fassnacht CD, Koopmans LVE, Sluse D, Blandford RD, Courbin F, Meylan G (2013) Two accurate time-delay distances from strong lensing: implications for cosmology. *ApJ* 766:70. doi:[10.1088/0004-637X/766/2/70](#)
- Suyu SH, Treu T, Hilbert S, Sonnenfeld A, Auger MW, Blandford RD, Collett T, Courbin F, Fassnacht CD, Koopmans LVE, Marshall PJ, Meylan G, Spiniello C, Tewes M (2014) Cosmology from gravitational lens time delays and Planck data. *ApJL* 788:L35. doi:[10.1088/2041-8205/788/2/L35](#). [arXiv:1306.4732](#)
- Tagore AS, Jackson N (2016) On the use of shapelets in modelling resolved, gravitationally lensed images. *MNRAS* 457:3066–3075. doi:[10.1093/mnras/stw057](#). [arXiv:1505.00198](#)
- Tak H, Mandel K, van Dyk DA, Kashyap VL, Meng XL, Siemiginowska A (2016) Bayesian estimates of astronomical time delays between gravitationally lensed stochastic light curves. [arXiv:1602.01462](#)
- Tewes M, Courbin F (2013) COSMOGRAIL: the COSmological MONitoring of GRAVItational lenses XI. Techniques for time delay measurement in presence of microlensing. *A A* 553:A120. doi:[10.1051/0004-6361/201220123](#). [arXiv:1208.5598](#)
- Tewes M, Courbin F, Meylan G, Kochanek CS, Eulaers E, Cantale N, Mosquera AM, Magain P, Van Winckel H, Sluse D, Cataldi G, Vörös D, Dye S (2013) COSMOGRAIL: the COSmological MONitoring of GRAVItational lenses. XIII. Time delays and 9-yr optical monitoring of the lensed quasar RX J1131–1231. *A A* 556:A22. doi:[10.1051/0004-6361/201220352](#). [arXiv:1208.6009](#)
- The Dark Energy Survey Collaboration, Abbott T, Abdalla FB, Allam S, Amara A, Annis J, Armstrong R, Bacon D, Banerji M, Bauer AH, Baxter E, Becker MR, Benoit-Lévy A, Bernstein RA, Bernstein GM, Bertin E, Blazek J, Bonnett C, Bridle SL, Brooks D, Bruderer C, Buckley-Geer E, Burke DL, Busha MT, Capozzi D, Carnero Rosell A, Carrasco Kind M, Carretero J, Castander FJ, Chang C, Clampitt J, Crocce M, Cunha CE, D'Andrea CB, da Costa LN, Das R, DePoy DL, Desai S, Diehl HT, Dietrich JP, Dodelson S, Doel P, Drlica-Wagner A, Efstathiou G, Eifler TF, Erickson B, Estrada J, Evrard AE, Fausti Neto A, Fernandez E, Finley DA, Flaugher B, Fosalba P, Friedrich O, Frieman J, Gangkofner C, Garcia-Bellido J, Gaztanaga E, Gerdes DW, Gruen D, Gruendl RA, Gutierrez G, Hartley W, Hirsch M, Honscheid K, Huff EM, Jain B, James DJ, Jarvis M, Kacprzak T, Kent S, Kirk D, Krause E, Kravtsov A, Kuehn K, Kuropatkin N, Kwan J, Lahav O, Leistedt B, Li TS, Lima M, Lin H, MacCrann N, March M, Marshall JL, Martini P, McMahon RG, Melchior P, Miller CJ, Miquel R, Mohr JJ, Neilsen E, Nichol RC, Nicola A, Nord B, Ogando R, Palmese A, Peiris HV, Plazas AA, Refregier A, Roe N, Romer AK, Roodman A, Rowe B, Rykoff ES, Sabiu C, Sadeh I, Sako M, Samuroff S, Sánchez C, Sanchez E, Seo H, Sevilla-Noarbe I, Sheldon E, Smith RC, Soares-Santos M, Sobreira F, Suchyta E, Swanson MEC, Tarle G, Thaler J, Thomas D, Troxel MA, Vikram V, Walker AR, Wechsler RH, Weller J, Zhang Y, Zuntz J (2015) Cosmology from cosmic shear with DES science verification data. [arXiv:1507.05552](#)

- Treu T (2010) Strong lensing by galaxies. *ARA A* 48:87–125. doi:[10.1146/annurev-astro-081309-130924](https://doi.org/10.1146/annurev-astro-081309-130924). [arXiv:1003.5567](https://arxiv.org/abs/1003.5567)
- Treu T, Ellis RS (2015) Gravitational lensing: Einsteins unfinished symphony. *Contemp Phys* 56(1):17–34. doi:[10.1080/00107514.2015.1006001](https://doi.org/10.1080/00107514.2015.1006001)
- Treu T, Koopmans LVE (2002a) The internal structure and formation of early-type galaxies: the gravitational lens system MG 2016+112 at $z = 1.004$. *ApJ* 575:87–94. doi:[10.1086/341216](https://doi.org/10.1086/341216). [arXiv:astro-ph/0202342](https://arxiv.org/abs/astro-ph/0202342)
- Treu T, Koopmans LVE (2002) The internal structure of the lens PG1115+080: breaking degeneracies in the value of the Hubble constant. *MNRAS* 337:L6–L10. doi:[10.1046/j.1365-8711.2002.06107.x](https://doi.org/10.1046/j.1365-8711.2002.06107.x). [arXiv:astro-ph/0210002](https://arxiv.org/abs/astro-ph/0210002)
- Treu T, Koopmans LVE (2004) Massive dark matter halos and evolution of early-type galaxies to $z \sim 1$. *ApJ* 611:739–760. doi:[10.1086/422245](https://doi.org/10.1086/422245). [arXiv:astro-ph/0401373](https://arxiv.org/abs/astro-ph/0401373)
- Treu T, Marshall PJ, Clowe D (2012) Resource letter GL-1: gravitational lensing. *Am J Phys* 80:753–763. doi:[10.1119/1.4726204](https://doi.org/10.1119/1.4726204). [arXiv:1206.0791](https://arxiv.org/abs/1206.0791)
- Treu T, Marshall PJ, Cyr-Racine FY, Fassnacht CD, Keeton CR, Linder EV, Moustakas LA, Bradac M, Buckley-Geer E, Collett T, Courbin F, Dobler G, Finley DA, Hjorth J, Kochanek CS, Komatsu E, Koopmans LVE, Meylan G, Natarajan P, Oguri M, Suyu SH, Tewes M, Wong KC, Zabludoff AI, Zaritsky D, Anguita T, Brunner RJ, Cabanac R, Falco EE, Fritz A, Seidel G, Howell DA, Giocoli C, Jackson N, Lopez S, Metcalf RB, Motta V, Verdugo T (2013) Dark energy with gravitational lens time delays. [arXiv:1306.1272](https://arxiv.org/abs/1306.1272)
- Treu T, Brammer G, Diego JM, Grillo C, Kelly PL, Oguri M, Rodney SA, Rosati P, Sharon K, Zitrin A, Balestra I, Bradač M, Broadhurst T, Caminha GB, Halkola A, Hoag A, Ishigaki M, Johnson TL, Karman W, Kawamata R, Mercurio A, Schmidt KB, Strolger LG, Suyu SH, Filippenko AV, Foley RJ, Jha SW, Patel B (2016) Refsdal meets popper: comparing predictions of the re-appearance of the multiply imaged supernova behind MACSJ1149.5+2223. *ApJ* 817:60. doi:[10.3847/0004-637X/817/1/60](https://doi.org/10.3847/0004-637X/817/1/60). [arXiv:1510.05750](https://arxiv.org/abs/1510.05750)
- Vanderriest C, Felenbok P, Schneider J, Wlerick G, Bijaoui A, Lelievre G (1982) The photometry of 0957 plus 561—detection of short-period variations. *A A* 110:L11–L14
- Vanderriest C, Schneider J, Herpe G, Chevreton M, Moles M, Wlerick G (1989) The value of the time delay $\Delta t(A, B)$ for the ‘double’ quasar 0957+561 from optical photometric monitoring. *A A* 215:1–13
- Vegetti S, Koopmans LVE (2009) Bayesian strong gravitational-lens modelling on adaptive grids: objective detection of mass substructure in galaxies. *MNRAS* 392:945–963. doi:[10.1111/j.1365-2966.2008.14005.x](https://doi.org/10.1111/j.1365-2966.2008.14005.x). [arXiv:0805.0201](https://arxiv.org/abs/0805.0201)
- Vegetti S, Koopmans LVE, Auger MW, Treu T, Bolton AS (2014) Inference of the cold dark matter substructure mass function at $z = 0.2$ using strong gravitational lenses. *MNRAS* 442:2017–2035. doi:[10.1093/mnras/stu943](https://doi.org/10.1093/mnras/stu943). [arXiv:1405.3666](https://arxiv.org/abs/1405.3666)
- Vuissoz C, Courbin F, Sluse D, Meylan G, Ibrahimov M, Asfandiyarov I, Stoops E, Eigenbrod A, Le Guillou L, van Winckel H, Magain P (2007) COSMOGRAIL: the COSmological MONitoring of GRAVItational lenses. V. The time delay in SDSS J1650+4251. *A A* 464:845–851. doi:[10.1051/0004-6361:20065823](https://doi.org/10.1051/0004-6361:20065823). [arXiv:astro-ph/0606317](https://arxiv.org/abs/astro-ph/0606317)
- Vuissoz C, Courbin F, Sluse D, Meylan G, Chantry V, Eulaers E, Morgan C, Eyler ME, Kochanek CS, Coles J, Saha P, Magain P, Falco EE (2008) COSMOGRAIL: the COSmological MONitoring of GRAVItational lenses. VII. Time delays and the Hubble constant from WFI J2033–4723. *A A* 488:481–490. doi:[10.1051/0004-6361:200809866](https://doi.org/10.1051/0004-6361:200809866). [arXiv:0803.4015](https://arxiv.org/abs/0803.4015)
- Walsh D, Carswell RF, Weymann RJ (1979) 0957 + 561 A, B—twin quasistellar objects or gravitational lens. *Nature* 279:381–384. doi:[10.1038/279381a0](https://doi.org/10.1038/279381a0)
- Warren SJ, Dye S (2003) Semilinear gravitational lens inversion. *ApJ* 590:673–682. doi:[10.1086/375132](https://doi.org/10.1086/375132). [arXiv:astro-ph/0302587](https://arxiv.org/abs/astro-ph/0302587)
- Weinberg DH, Mortonson MJ, Eisenstein DJ, Hirata C, Riess AG, Rozo E (2013) Observational probes of cosmic acceleration. *Phys. Rep.* 530:87–255. doi:[10.1016/j.physrep.2013.05.001](https://doi.org/10.1016/j.physrep.2013.05.001). [arXiv:1201.2434](https://arxiv.org/abs/1201.2434)
- Wong KC, Keeton CR, Williams KA, Momcheva IG, Zabludoff AI (2011) The effect of environment on shear in strong gravitational lenses. *ApJ* 726:84. doi:[10.1088/0004-637X/726/2/84](https://doi.org/10.1088/0004-637X/726/2/84). [arXiv:1011.2504](https://arxiv.org/abs/1011.2504)
- Wucknitz O (2002) Degeneracies and scaling relations in general power-law models for gravitational lenses. *MNRAS* 332:951–961. doi:[10.1046/j.1365-8711.2002.05426.x](https://doi.org/10.1046/j.1365-8711.2002.05426.x). [arXiv:astro-ph/0202376](https://arxiv.org/abs/astro-ph/0202376)
- Wucknitz O, Biggs AD, Browne IWA (2004) Models for the lens and source of B0218+357: a LENS CLEAN approach to determine H_0 . *MNRAS* 349:14–30. doi:[10.1111/j.1365-2966.2004.07514.x](https://doi.org/10.1111/j.1365-2966.2004.07514.x). [arXiv:astro-ph/0312263](https://arxiv.org/abs/astro-ph/0312263)

- Xu D, Sluse D, Schneider P, Springel V, Vogelsberger M, Nelson D, Hernquist L (2016) Lens galaxies in the Illustris simulation: power-law models and the bias of the Hubble constant from time delays. *MNRAS* 456:739–755. doi:[10.1093/mnras/stv2708](https://doi.org/10.1093/mnras/stv2708). [arXiv:1507.07937](https://arxiv.org/abs/1507.07937)
- Xu DD, Mao S, Wang J, Springel V, Gao L, White SDM, Frenk CS, Jenkins A, Li G, Navarro JF (2009) Effects of dark matter substructures on gravitational lensing: results from the Aquarius simulations. *MNRAS*, p 1108. doi:[10.1111/j.1365-2966.2009.15230.x](https://doi.org/10.1111/j.1365-2966.2009.15230.x). [arXiv:0903.4559](https://arxiv.org/abs/0903.4559)